Stability of a magnon Bose-Einstein condensate

Supervisors: Rembert Duine and Benedetta Flebus

C.J. van Diepen

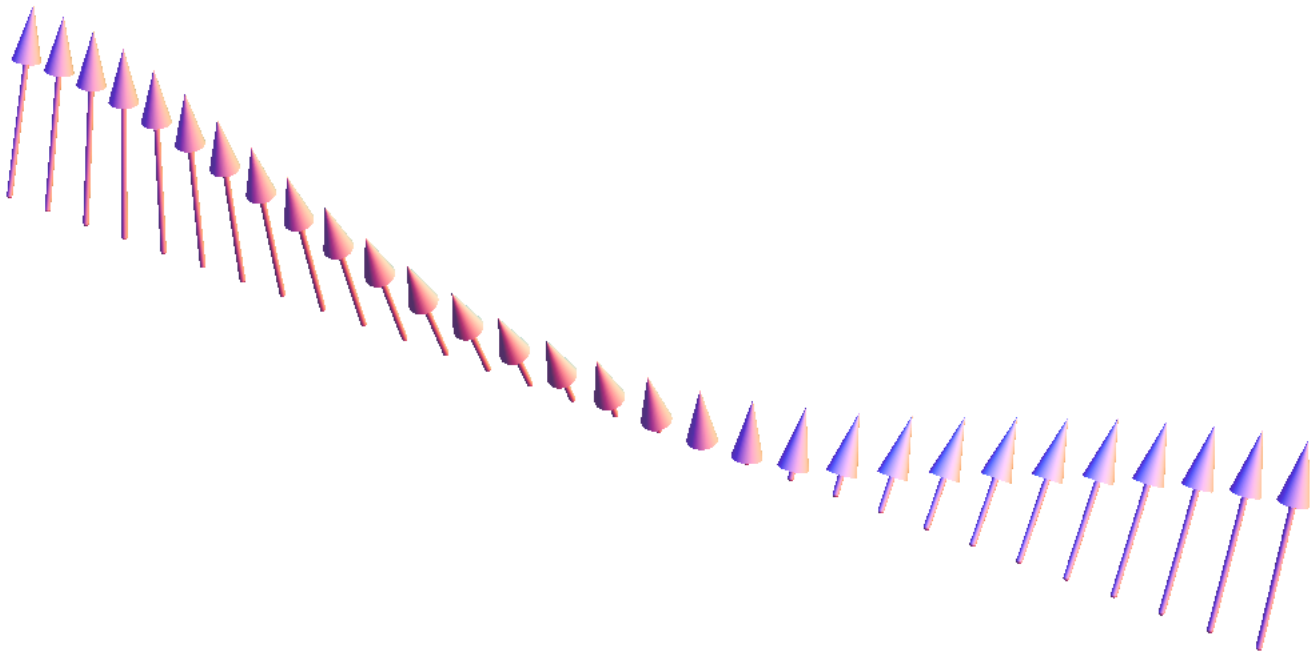

Master's thesis presented for the degree of
Master of Science

Institute for Theoretical Physics
Utrecht University
Netherlands
January 26, 2016

Abstract

A quantized spin wave, a magnon, behaves as a weakly-interacting bosonic particle. In recent experiments [Demokritov *et al.*, 2006] a Bose-Einstein condensate (BEC) of magnons has been realized in a thin film of Yttrium-iron-garnet (YIG) at room temperature by using a technique called parametric pumping. The interactions within this condensate are investigated, because it has been suggested that they are attractive [Tupitsyn *et al.*, 2008], hence the condensate could be unstable and collapse. The influence of relaxation and parametric pumping on the stability of the BEC, however are not yet well understood. In this thesis we find as estimate for the critical density, $10^5\,\mathrm{cm}^{-2} < n_{\mathrm{crit}} < 10^7\,\mathrm{cm}^{-2}$, for a magnon BEC in YIG. We also find that increased pumping tends to make the BEC unstable and that in general increased damping tends to make the BEC stable.

Contents

Chapter 1

Introduction

1.1 Research area

In nature we can distinguish between two major classes of particles, bosons and fermions. One of the main differences between these two is that bosons can occupy the same state but fermions have to obey the Pauli exclusion principle, which precludes them from occupying the same state. A result of this difference is that only bosons can undergo a phase transition into a Bose-Einstein condensate (BEC), the state in which the ground state is macroscopically occupied (see Section 1.2), at sufficiently high density and low temperature.

The existence of a Bose Einstein condensate was already theoretically predicted in 1924 by Satyendra Bose [1] and Albert Einstein [2, 3] in an ideal Bose gas of non-interacting particles. It took until 1995 before the first weakly-interacting BEC was experimentally realized [4]. The first BEC's were realized by trapping a dilute gas of atoms at extremely low temperatures, i.e. at a few nanokelvin.

In this thesis we are not dealing with atoms but instead with spin waves. A spin wave (see Section 1.3) is a propagating disturbance in a magnetically ordered system. In the groundstate of a ferromagnet all spins are aligned. When one of the spins is deflected from its original direction, the magnetic field associated with this spin is changed, its neighboring spins will feel this change of magnetic field and will also be deflected in order to become aligned again, and so on, producing a propagating wave of deflected spins, a spin wave. The quantized spin wave, the magnon, was introduced in 1940 by Holstein and Primakoff [5]. They predicted that magnons should behave as bosonic particles. This gives rise to the question whether or not it is possible to produce a BEC of magnons. In 2006 the first observation of a

BEC of magnons at room temperature was claimed [6]. It was produced in a thin film of a ferromagnetic material called Yttrium-iron-garnet (YIG). This material is very suitable for the experimental investigation of a magnon BEC because of two important reasons. First, because it allows for the creation of additional magnons with energy values near the ground energy by using parametric pumping, such that even at room temperature densities can be reached that are sufficient to achieve the BEC transition. Second, it has very low Gilbert damping, hence a very long spin-lattice relaxation time, thus it allows for magnons to live a lot longer then that it takes for magnons to thermalize through scattering mechanisms, hence allowing magnons to relax into a quasi-equilibrium state with nonzero chemical potential which facilitated BEC formation. Motivated by these and other experiments, a research area called "magnonics" has developed because of the technological applications of magnonic devices in data storage and information processing [7].

In a paper [8] published in 2008 the stability of magnon BEC's in thin films of YIG realized in experiments has been investigated. The study of the stability and possible collapse of a BEC has some similarity with that of collapse of a neutron star due to its own gravity. Because if there are attractive interactions in a BEC it might also collapse due to these interactions. This has also been studied in the context of atomic condensates, see e.g. Ref. [9]. The theoretical study mentioned above, ignored the effects of parametric pumping and damping. In this thesis we study the stability of these BEC's and consider dynamics by using a Gaussian ansatz for the BEC wavefunction and include the effects of the Gilbert damping and the parametric pumping on the stability of the BEC. It is organized as followed. In Chapter 2 we set up a theoretical framework to compute the dispersion relation for the lowest energy band and derive the magnon quantum many-body Hamiltonian up to fourth order in the magnon operators. In Chapter 3 we use this framework in order to obtain results for the dispersion relation and interaction, and derive an estimate for the critical density of the magnon BEC. In Chapter 4 we study the dynamics of the BEC. We use a Gaussian ansatz for the wavefunction of the BEC, derive the equations of motion, and study the influence of Gilbert damping and parametric pumping on the stability of the BEC.

1.2 Bose-Einstein condensation

Bose-Einstein condensation is one of the most fascinating phenomena in quantum physics. It is a state of matter with the main characteristic that the number of particles in the ground state is on the same order of magni-

tude as the total number of particles. The first BEC's in experiments were realized by trapping a dilute ultracold atomic gas [4]. In order to get a better understanding of Bose-Einstein condensation we consider the Bose-Einstein distribution

$$\langle N \rangle = \sum_{\mathbf{k}} N_{\mathbf{k}} = \sum_{\mathbf{k}} \frac{1}{e^{(\hbar\omega_{\mathbf{k}} - \mu)/k_B T} - 1}, \tag{1.2.1}$$

with N the total number of particles, $N_{\mathbf{k}}$ the number of particles in the state with energy $\hbar\omega_{\mathbf{k}}$, μ the chemical potential, k_B the Boltzmann constant and T the temperature. This distribution describes what the probability is of finding a particle with energy $\hbar\omega_{\mathbf{k}}$ in a non-interacting ideal Bose gas at temperature T and with chemical potential μ. If $\mu = \hbar\omega_{\mathbf{k}_0}$, this distribution is ill-defined for $\mathbf{k} = \mathbf{k}_0$, with $\mathbf{k}_0$ the minimum of the single particle energy $\hbar\omega_{\mathbf{k}}$. Thus in order for the system to become a BEC, hence $\langle N_{\mathbf{k}_0} \rangle \sim \langle N \rangle$, the chemical potential must be as high as the minimum of the single particle energy.

Let us consider a system with a fixed number of bosonic particles. If we lower the temperature of the system then for the number of particles to remain constant the chemical potential will increase until $\mu = \hbar\omega_{\mathbf{k}_0}$, as can be seen from eqn. (1.2.1). By further lowering the temperature particles in excited states will be forced into lower energy states, causing $\langle N_{\mathbf{k}_0} \rangle$ to increase, hence forming a BEC. For a system with fixed temperature it is also possible to achieve a BEC but then the number of particles has to be raised. Looking at eqn. (1.2.1) we see that then the chemical potential will also increase, hence eventually a BEC can form.

1.3 Magnon

The ground state of a ferromagnet is the state in which all spins are aligned with the magnetic field. A spin wave corresponds to the excited state in which a deviation of the spin from the direction of the magnetic field at a certain lattice site propagates through the material by deflecting neighboring spins, which in turn deflect neighboring spins and so on. A characteristic property of spin waves is that the deflected spins precess around the direction of the magnetic field until they return to their initial position due to dissipation into the lattice. In Fig. 1.1 a schematic presentation of the ground state of a ferromagnet and of a spin wave are shown.

From quantum mechanics it is well-known that by quantizing a wave one obtains the corresponding particle, as for example a photon corresponds to a quantized electromagnetic wave. The quantized spin wave is called a

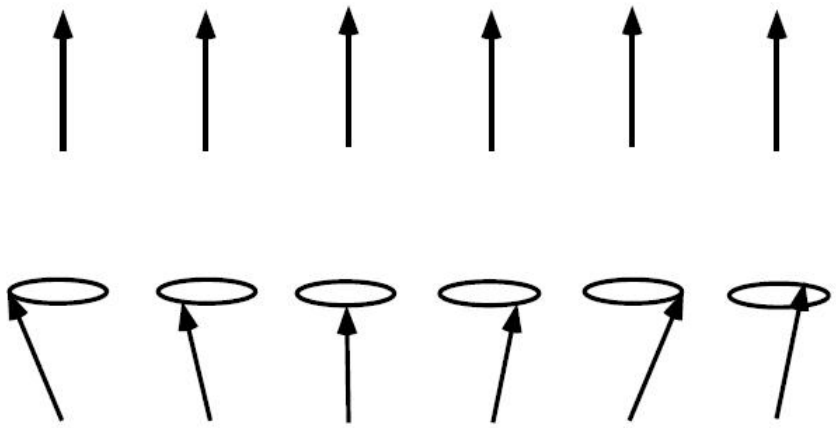

Figure 1.1: The upper row corresponds to spins in the ground state of a ferromagnet, while the lower row corresponds to a spin wave.

magnon. Note that a magnon is not an elementary particle but is a quasi-particle, because it is the particle-like description of the collective excitation of the spins of unit cells of an underlying material.

1.4 Magnon BEC

In the experiment described in Section 1.1 the number of magnons is not conserved, because they dissipate to the lattice via spin-orbit coupling. In thermodynamic equilibrium the chemical potential is thus equal to zero. However $\hbar\omega_{\mathbf{k}_0}$ is not equal to zero, as will later be shown. By using parametric pumping, magnons with energy near the energy minimum can be created and the chemical potential of the magnon gas can be raised in order to bring the system close to the condition for BEC transition. Even for a system at room temperature it can be possible to achieve a BEC if the number of magnons injected into the system is high enough. Because the spin-lattice relaxation time of YIG films can be above $1\,\mu$s, and the thermalization time can be as low as $100 - 200\,$ns it is possible to realize a quasi-equilibrium state for the magnon gas, hence making it possible to create a magnon BEC. If the interactions in a BEC are attractive the condensate can become unstable and the magnon gas will tend to collapse.

Chapter 2

Magnon-magnon interactions in a thin film of YIG

In this chapter we derive the magnon quantum many-body Hamiltonian up to fourth order in the magnon operators. This is the basis for our study of the stability of a magnon Bose-Einstein condensate in a film of YIG at room temperature.

2.1 The spin Hamiltonian

Let us consider a film of YIG at room temperature and focus on the lowest magnon band, because this is the band that is most important on the energy scales relevant to experiments [6]. Though the crystal structure of YIG is rather complex, at this low-energy scale, i.e. for longer wavelengths, the properties of YIG can be described by an effective spin quantum Heisenberg ferromagnet on a cubic lattice with lattice spacing $a = 12.376$ Å. The effective spin Hamiltonian contains exchange and dipole interaction, and reads as [8, 10, 11, 12]

$$H_{\text{spin}} = -\frac{1}{2}\sum_{i,j}\sum_{\alpha,\beta}[J_{ij}\delta^{\alpha\beta} + D_{ij}^{\alpha\beta}]S_i^\alpha S_j^\beta - B\sum_i S_i^z, \tag{2.1.1}$$

where $\alpha, \beta \in \{x, y, z\}$ label the spatial components and $i, j \in \{1, \ldots, N\}$, with N being the total number of lattice sites, indicate the lattice site. S_i^α is the α-component of the spin operator at lattice site i. The third term contains $B = \mu B_e$, which denotes the energy associated to a static magnetic field, B_e, that is pointing in the positive z-direction with $\mu = g\mu_B$ the magnetic moment, where $g = 2$ is the effective g-factor and μ_B the Bohr magneton. The exchange interaction, J_{ij}, is equal to $J \approx 1.29$ K if i and j denote

lattice sites that are nearest neighbors and is zero otherwise [8]. The matrix elements for the dipole interaction are given as

$$D_{ij}^{\alpha\beta} = (1-\delta_{ij})\frac{\mu^2}{|\mathbf{R}_{ij}|^3}[3\hat{R}_{ij}^{\alpha}\hat{R}_{ij}^{\beta} - \delta^{\alpha\beta}] \tag{2.1.2}$$

with $\mathbf{R}_{ij} = \mathbf{R}_i - \mathbf{R}_j$ and $\hat{R}_{ij} = \frac{\mathbf{R}_{ij}}{|\mathbf{R}_{ij}|}$, where $\mathbf{R}_i$ is the position of the i-th spin.

2.2 Holstein-Primakoff transformation

To go from the effective spin Hamiltonian in eqn. (2.1.1) to a Hamiltonian of a quantum many-body system involving magnons we will perform a Holstein-Primakoff transformation [5]. An additional advantage of the Holstein-Primakoff transformation is that it allows a Taylor series expansion in spin deviations that converges quickly for deviations that are relatively small compared with the total spin. This expansion allows us to separate terms that have a different order in magnon creation and annihilation operators.

First let us introduce the spin raising and lowering operators

$$S_i^+ = S_i^x + iS_i^y, \qquad S_i^- = S_i^x - iS_i^y, \tag{2.2.1}$$

$$\Rightarrow S_i^x = \frac{1}{2}\left(S_i^+ + S_i^-\right), \qquad S_i^y = \frac{i}{2}\left(S_i^- - S_i^+\right). \tag{2.2.2}$$

By plugging eqn. (2.2.2) into eqn. (2.1.1) we can express the Hamiltonian in terms of spin raising and lowering operators, and the z-component of the spin operator.

The Holstein-Primakoff transformation allows us to rewrite the spin raising and lowering operators and the z-component of the spin operator as

$$S_i^+ = \sqrt{2S}\sqrt{1 - \frac{b_i^\dagger b_i}{2S}}b_i, \tag{2.2.3a}$$

$$S_i^- = \sqrt{2S}b_i^\dagger\sqrt{1 - \frac{b_i^\dagger b_i}{2S}}, \tag{2.2.3b}$$

$$S_i^z = S - b_i^\dagger b_i. \tag{2.2.3c}$$

with respectively b_i and $b_i^\dagger$ a magnon annihilation and a magnon creation operator, i.e.,

$$[b_i, b_j^\dagger] = \delta_{ij}. \tag{2.2.4}$$

Note that the magnon creation and annihilation operator obey a bosonic commutation relation, hence magnons are bosons. Here, $S = \frac{M_S a^3}{\mu}$ is the effective spin with M_S the saturation magnetization. The saturation magnetization of YIG at room temperature is $M_S = \frac{1750}{4\pi}$ G, hence $S \approx 14.2$ [8].

We perform a Taylor expansion in $\frac{b_i^\dagger b_i}{2S}$: this corresponds to focusing on spin deviations that are relatively small compared to the total spin. The Taylor expansion allows us to write the raising and lowering spin operators as

$$S_i^+ = \sqrt{2S}\left[b_i - \frac{b_i^\dagger b_i b_i}{4S} + \dots\right], \qquad S_i^- = \sqrt{2S}\left[b_i^\dagger - \frac{b_i^\dagger b_i^\dagger b_i}{4S} + \dots\right]. \quad (2.2.5)$$

By plugging eqn. (2.2.5) into eqn. (2.2.2) we obtain

$$S_i^x = \sqrt{\frac{S}{2}}\left[b_i + b_i^\dagger - \frac{b_i^\dagger b_i b_i}{4S} - \frac{b_i^\dagger b_i^\dagger b_i}{4S} + \dots\right], \quad (2.2.6)$$

$$S_i^y = i\sqrt{\frac{S}{2}}\left[b_i^\dagger - b_i - \frac{b_i^\dagger b_i^\dagger b_i}{4S} + \frac{b_i^\dagger b_i b_i}{4S} + \dots\right] \quad (2.2.7)$$

By plugging eqn. (2.2.6), eqn. (2.2.7) and eqn. (2.2.3c) into eqn. (2.1.1) we obtain the quantum many-body Hamiltonian.

2.3 The many-body Hamiltonian

We consider the quantum many-body Hamiltonian up to fourth order in the magnon operators to get a better understanding of the effects of interactions on the stability of a magnon Bose-Einstein condensate and contributions from the fourth order term are dominant over higher order terms. The Hamiltonian can then be written as

$$H = H_0 + H_2 + H_3 + H_4, \quad (2.3.1)$$

where the subindices correspond to the order of magnon operators. Actually, in the derivation of the expansion of the Hamiltonian in terms of magnon operators there also appears a term linear in the magnon operators. The presence of this term might indicate that the assumed ground state spin configuration is not correct [13]. By requiring that the linear order term, which is not physical, is zero one can obtain the correct angles for the spins in the ground state configuration. In eqn. (2.3.1) we have neglected H_1

because its contribution is small compared to the other terms. By plugging eqn. (2.2.5) in eqn. (2.2.2) and plugging the result from that in eqn. (2.1.1) we obtain the zeroth-order term, H_0, as

$$H_0 = -\frac{S^2}{2}\sum_{i,j}\left[J_{ij} + D_{ij}^{zz}\right] - NSB. \tag{2.3.2}$$

While the quadratic term, H_2, is

$$H_2 = \sum_{i,j}\left[A_{ij}b_i^\dagger b_j + \left(\frac{B_{ij}}{2}b_i b_j + h.c.\right)\right], \tag{2.3.3}$$

with A_{ij} and B_{ij} given as

$$A_{ij} = B\delta_{ij} - S\left[J_{ij} - \delta_{ij}\sum_n J_{in}\right] - S\left[\frac{D_{ij}^{xx} + D_{ij}^{yy}}{2} - \delta_{ij}\sum_n D_{in}^{zz}\right], \tag{2.3.4a}$$

$$B_{ij} = -\frac{S}{2}\left[D_{ij}^{xx} - 2iD_{ij}^{xy} - D_{ij}^{yy}\right]. \tag{2.3.4b}$$

Note that B without subindices is the external magnetic field. The cubic term, H_3, reads as

$$H_3 = \sqrt{\frac{S}{2}}\sum_{i,j}\left[\left(D_{ij}^{xz} + iD_{ij}^{yz}\right)\left(b_i^\dagger b_j^\dagger b_j + \frac{1}{4}b_i^\dagger b_i^\dagger b_i\right) + h.c.\right]. \tag{2.3.5}$$

The quartic term, H_4, is

$$\begin{aligned} H_4 = -\frac{1}{2}\sum_{i,j}\Bigg[& J_{ij}\left(b_i^\dagger b_i b_j^\dagger b_j - \frac{1}{2}(b_i^\dagger b_j^\dagger b_j b_j + h.c.)\right) \\ & - \frac{1}{4}\left(\left(D_{ij}^{xx} + 2iD_{ij}^{xy} - D_{ij}^{yy}\right)b_i^\dagger b_j^\dagger b_j^\dagger b_j + h.c.\right) \\ & - \frac{1}{4}\left(\left(D_{ij}^{xx} + D_{ij}^{yy}\right)\left(b_i^\dagger b_j^\dagger b_j b_j + h.c.\right)\right) \\ & - D_{ij}^{zz}b_i^\dagger b_i b_j^\dagger b_j\Bigg]. \end{aligned} \tag{2.3.6}$$

2.4 The dispersion relation

In order to obtain the dispersion relation for the lowest magnon band we perform a Fourier transformation of the Hamiltonian. The thickness, d, of the film of YIG is relatively small compared to its width and length, hence we can

approximate the latter two to be infinite. Since there is discrete translational invariance in the yz-plane, we perform a partial Fourier transform, namely only for the y- and z-direction. We set $\mathbf{R}_i = (x_i, \mathbf{r}_i)$, with $\mathbf{r}_i = (y_i, z_i)$ and introduce the two-dimensional wave-vector $\mathbf{k} = (k_y, k_z)$. The partial Fourier transformation yields

$$b_i = \frac{1}{\sqrt{N_y N_z}} \sum_{\mathbf{k}} b_{\mathbf{k}}(x_i) e^{i\mathbf{k}\cdot\mathbf{r}_i}, \qquad b_i^\dagger = \frac{1}{\sqrt{N_y N_z}} \sum_{\mathbf{k}} b_{\mathbf{k}}^\dagger(x_i) e^{-i\mathbf{k}\cdot\mathbf{r}_i}, \tag{2.4.1}$$

with N_y, N_z respectively the number of layers of lattice sites in the y-direction and in the z-direction.

We use the uniform mode approximation, i.e. we ignore that the system is not translation-invariant in the x-direction and approximate its eigenfunctions by plane-waves. The validity of this analytical approximation has been studied in Ref. [10] and in general it shows quite good agreement with experimental results. We look at the lowest magnon band, $k_x = 0$, hence approximate as

$$b_{\mathbf{k}}(x_i) = \frac{1}{\sqrt{N_x}} b_{\mathbf{k}}, \qquad b_{\mathbf{k}}^\dagger(x_i) = \frac{1}{\sqrt{N_x}} b_{\mathbf{k}}^\dagger. \tag{2.4.2}$$

eqn. (2.4.2) combined with eqn. (2.4.1) yields

$$b_i = \frac{1}{\sqrt{N}} \sum_{\mathbf{k}} b_{\mathbf{k}} e^{i\mathbf{k}\cdot\mathbf{r}_i}, \qquad b_i^\dagger = \frac{1}{\sqrt{N}} \sum_{\mathbf{k}} b_{\mathbf{k}}^\dagger e^{-i\mathbf{k}\cdot\mathbf{r}_i} \tag{2.4.3}$$

and accordingly

$$A_{ij} = \frac{1}{N} \sum_{\mathbf{k}} A_{\mathbf{k}} e^{i\mathbf{k}\cdot(\mathbf{r}_i - \mathbf{r}_j)}, \qquad B_{ij} = \frac{1}{N} \sum_{\mathbf{k}} B_{\mathbf{k}} e^{i\mathbf{k}\cdot(\mathbf{r}_i - \mathbf{r}_j)}, \tag{2.4.4}$$

where we have used that A_{ij} and B_{ij} only depend on the difference $\mathbf{r}_i - \mathbf{r}_j$. The explicit calculation of $A_{\mathbf{k}}$ and $B_{\mathbf{k}}$ follows in the next section. However, for convenience we will use that $A_{\mathbf{k}}$ and $B_{\mathbf{k}}$ turn out to be real. Let us focus on the quadratic term in the Hamiltonian, in order to obtain the dispersion relation. By plugging eqn. (2.4.3) and eqn. (2.4.4) into eqn. (2.3.3) we obtain the quadratic term as

$$\begin{aligned} H_2 &= \sum_{\mathbf{k}} \left[A_{\mathbf{k}} b_{\mathbf{k}}^\dagger b_{\mathbf{k}} + \frac{1}{2} B_{\mathbf{k}} b_{-\mathbf{k}} b_{\mathbf{k}} + \frac{1}{2} B_{\mathbf{k}} b_{\mathbf{k}}^\dagger b_{-\mathbf{k}}^\dagger \right] \\ &= \sum_{\mathbf{k}} \begin{pmatrix} b_{\mathbf{k}}^\dagger & b_{-\mathbf{k}} \end{pmatrix} \begin{pmatrix} A_{\mathbf{k}} & \frac{1}{2} B_{\mathbf{k}} \\ \frac{1}{2} B_{\mathbf{k}} & 0 \end{pmatrix} \begin{pmatrix} b_{\mathbf{k}} \\ b_{-\mathbf{k}}^\dagger \end{pmatrix}. \end{aligned} \tag{2.4.5}$$

In order to obtain the dispersion relation we need to diagonalize eqn. (2.4.5) via a Bogoliubov transformation, i.e.

$$\begin{pmatrix} b_{\mathbf{k}} \\ b^{\dagger}_{-\mathbf{k}} \end{pmatrix} = \begin{pmatrix} u^{*}_{\mathbf{k}} & -v_{\mathbf{k}} \\ -v^{*}_{\mathbf{k}} & u_{\mathbf{k}} \end{pmatrix} \begin{pmatrix} a_{\mathbf{k}} \\ a^{\dagger}_{-\mathbf{k}} \end{pmatrix}, \tag{2.4.6}$$

where $u_{\mathbf{k}}$ and $v_{\mathbf{k}}$ are complex numbers, and $a_{\mathbf{k}}$ and $a^{\dagger}_{\mathbf{k}}$ are new operators. From eqn. (2.4.6) we obtain that

$$b^{\dagger}_{\mathbf{k}} = u_{\mathbf{k}} a^{\dagger}_{\mathbf{k}} - v^{*}_{\mathbf{k}} a_{-\mathbf{k}}, \qquad b^{\dagger}_{\mathbf{k}} = -v^{*}_{-\mathbf{k}} a_{-\mathbf{k}} + u_{-\mathbf{k}} a^{\dagger}_{\mathbf{k}}, \tag{2.4.7}$$

which combined yield that $u_{\mathbf{k}} = u_{-\mathbf{k}}$ and $v_{\mathbf{k}} = v_{-\mathbf{k}}$. As usual, we demand that the operators $a_{\mathbf{k}}$ and $a^{\dagger}_{\mathbf{k}}$ obey the same commutation relations as $b_{\mathbf{k}}$ and $b^{\dagger}_{\mathbf{k}}$, i.e. $a_{\mathbf{k}}$ and $a^{\dagger}_{\mathbf{k}}$ also are bosonic operators. By solving $[b_{\mathbf{k}}, b^{\dagger}_{\mathbf{k}'}] = [a_{\mathbf{k}}, a^{\dagger}_{\mathbf{k}'}]$ for $u_{\mathbf{k}}$ and $v_{\mathbf{k}}$ we obtain the constraint

$$|u_{\mathbf{k}}|^2 - |v_{\mathbf{k}}|^2 = 1. \tag{2.4.8}$$

Requiring that the quadratic part of the Hamiltonian becomes diagonal by performing the Bogoliubov transformation yields that the Bogoliubov coefficients are real and must obey

$$B_{\mathbf{k}} v^2_{\mathbf{k}} + B_{\mathbf{k}} u^2_{\mathbf{k}} - 2A_{\mathbf{k}} u_{\mathbf{k}} v_{\mathbf{k}} = 0. \tag{2.4.9}$$

By using the quadratic formula on eqn. (2.4.9) and using eqn. (2.4.8) we obtain that

$$u_{\mathbf{k}} = \sqrt{\frac{A_{\mathbf{k}} + \hbar\omega_{\mathbf{k}}}{2\hbar\omega_{\mathbf{k}}}}, \qquad v_{\mathbf{k}} = \sqrt{\frac{A_{\mathbf{k}} - \hbar\omega_{\mathbf{k}}}{2\hbar\omega_{\mathbf{k}}}}, \tag{2.4.10}$$

with

$$\hbar\omega_{\mathbf{k}} = \sqrt{A^2_{\mathbf{k}} - B^2_{\mathbf{k}}}. \tag{2.4.11}$$

By plugging eqn. (2.4.10) into eqn. (2.4.6) and inserting that into eqn. (2.4.5) combined with eqn. (2.4.11) yields

$$H_2 = \sum_{\mathbf{k}} \left[\hbar\omega_{\mathbf{k}} a^{\dagger}_{\mathbf{k}} a_{\mathbf{k}} + \frac{1}{2}(\hbar\omega_{\mathbf{k}} - A_{\mathbf{k}}) \right]. \tag{2.4.12}$$

Leaving out the constant terms yields the second order term as

$$H_2 = \sum_{\mathbf{k}} \hbar\omega_{\mathbf{k}} a^{\dagger}_{\mathbf{k}} a_{\mathbf{k}}. \tag{2.4.13}$$

2.5 The dipole interaction

In order to obtain $A_{\mathbf{k}}$ and $B_{\mathbf{k}}$ explicitly we need to calculate the Fourier transform of the exchange interaction and of the dipole interaction term. The Fourier transform of the exchange interaction of the lowest magnon band is

$$J_{\mathbf{k}} = 2J\left(1 + \cos(k_y a) + \cos(k_z a)\right). \tag{2.5.1}$$

The Fourier transform of the dipole interaction in eqn. (2.1.2) is

$$D_{\mathbf{k}}^{\alpha\beta} = \mu^2 \sum_{x_{ij},y_{ij},z_{ij}} \frac{e^{-i|\mathbf{k}|(y_{ij}\sin\theta_{\mathbf{k}} + z_{ij}\cos\theta_{\mathbf{k}})}}{(x_{ij}^2 + y_{ij}^2 + z_{ij}^2)^{\frac{5}{2}}} [3\hat{R}_{ij}^{\alpha}\hat{R}_{ij}^{\beta} - \delta^{\alpha\beta}]. \tag{2.5.2}$$

Where the in-plane wave-vector is parametrized as $\mathbf{k} = |\mathbf{k}|\left(\sin\theta_{\mathbf{k}}\mathbf{e}_y + \cos\theta_{\mathbf{k}}\mathbf{e}_z\right)$. Let us replace the sum in eqn. (2.5.2) by an integration as

$$\sum_{x_{ij},y_{ij},z_{ij}} \to \frac{1}{a^3}\int_{-\frac{d}{2}}^{\frac{d}{2}}\int_{-\infty}^{\infty}\int_{\infty}^{\infty} \mathrm{d}x\mathrm{d}y\mathrm{d}z. \tag{2.5.3}$$

By going to cylindrical coordinates we obtain

$$D_{\mathbf{k}}^{xx} = \frac{\mu^2}{a^3}\int \frac{e^{-i|\mathbf{k}|r\cos(\theta-\theta_{\mathbf{k}})}}{(x^2+r^2)^{\frac{3}{2}}}\left(\frac{3x^2}{x^2+r^2} - 1\right)\mathrm{d}\theta\mathrm{d}r\mathrm{d}x, \tag{2.5.4a}$$

$$D_{\mathbf{k}}^{yy} = \frac{\mu^2}{a^3}\int \frac{e^{-i|\mathbf{k}|r\cos(\theta-\theta_{\mathbf{k}})}}{(x^2+r^2)^{\frac{3}{2}}}\left(\frac{3r^2\sin^2\theta}{x^2+r^2} - 1\right)\mathrm{d}\theta\mathrm{d}r\mathrm{d}x, \tag{2.5.4b}$$

$$D_{\mathbf{k}}^{zz} = \frac{\mu^2}{a^3}\int \frac{e^{-i|\mathbf{k}|r\cos(\theta-\theta_{\mathbf{k}})}}{(x^2+r^2)^{\frac{3}{2}}}\left(\frac{3r^2\cos^2\theta}{x^2+r^2} - 1\right)\mathrm{d}\theta\mathrm{d}r\mathrm{d}x, \tag{2.5.4c}$$

$$D_{\mathbf{k}}^{xy} = \frac{\mu^2}{a^3}\int \frac{e^{-i|\mathbf{k}|r\cos(\theta-\theta_{\mathbf{k}})}}{(x^2+r^2)^{\frac{3}{2}}}\frac{3xr\sin\theta}{x^2+r^2}\mathrm{d}\theta\mathrm{d}r\mathrm{d}x, \tag{2.5.4d}$$

$$D_{\mathbf{k}}^{xz} = \frac{\mu^2}{a^3}\int \frac{e^{-i|\mathbf{k}|r\cos(\theta-\theta_{\mathbf{k}})}}{(x^2+r^2)^{\frac{3}{2}}}\frac{3xz\cos\theta}{x^2+r^2}\mathrm{d}\theta\mathrm{d}r\mathrm{d}x, \tag{2.5.4e}$$

$$D_{\mathbf{k}}^{yz} = \frac{\mu^2}{a^3}\int \frac{e^{-i|\mathbf{k}|r\cos(\theta-\theta_{\mathbf{k}})}}{(x^2+r^2)^{\frac{3}{2}}}\frac{3r^2\sin\theta\cos\theta}{x^2+r^2}\mathrm{d}\theta\mathrm{d}r\mathrm{d}x. \tag{2.5.4f}$$

Let us perform explicitly the integrations in eqn. (2.5.4). Integrating in the order θ, x and as last r yields

$$D_{\mathbf{k}}^{xx} = -\frac{4\pi\mu^2}{a^3} e^{-\frac{|\mathbf{k}|d}{2}}, \tag{2.5.5a}$$

$$D_{\mathbf{k}}^{yy} = \frac{4\pi\mu^2}{a^3}\left(\frac{1}{2} + \left(e^{-\frac{|\mathbf{k}|d}{2}} - 1\right)\sin^2\theta_{\mathbf{k}}\right), \tag{2.5.5b}$$

$$D_{\mathbf{k}}^{zz} = \frac{4\pi\mu^2}{a^3}\left(\frac{1}{2} + \left(e^{-\frac{|\mathbf{k}|d}{2}} - 1\right)\cos^2\theta_{\mathbf{k}}\right), \tag{2.5.5c}$$

$$D_{\mathbf{k}}^{xy} = 0, \tag{2.5.5d}$$

$$D_{\mathbf{k}}^{xz} = 0, \tag{2.5.5e}$$

$$D_{\mathbf{k}}^{yz} = \frac{2\pi\mu^2}{a^3}\left(e^{-\frac{|\mathbf{k}|d}{2}} - 1\right)\sin(2\theta_{\mathbf{k}}). \tag{2.5.5f}$$

Actually, so far we have ignored the fact that the dipole interaction does not lead to a self interaction. In order to account for the factor $(1 - \delta_{ij})$ in the dipole term in eqn. (2.1.2) we subtract the contribution from integrating $e^{-i\mathbf{kr}} D_{ij}^{\alpha\beta}$ over an infinitesimally small sphere around the origin to the dipole terms in eqn. (2.5.5). That contribution is

$$D_{\mathbf{k}}^{xx} = -\frac{4\pi\mu^2}{3a^3}, \tag{2.5.6a}$$

$$D_{\mathbf{k}}^{yy} = \frac{2\pi\mu^2}{3a^3}, \tag{2.5.6b}$$

$$D_{\mathbf{k}}^{zz} = \frac{2\pi\mu^2}{3a^3}, \tag{2.5.6c}$$

$$D_{\mathbf{k}}^{xy} = 0, \tag{2.5.6d}$$

$$D_{\mathbf{k}}^{xz} = 0, \tag{2.5.6e}$$

$$D_{\mathbf{k}}^{yz} = 0. \tag{2.5.6f}$$

Subtracting the quantities in eqn. (2.5.6) from the values in eqn. (2.5.5) yields

$$D_{\mathbf{k}}^{xx} = \frac{4\pi\mu^2}{a^3}\left(\frac{1}{3} - f_{\mathbf{k}}\right), \tag{2.5.7a}$$

$$D_{\mathbf{k}}^{yy} = \frac{4\pi\mu^2}{3a^3}\left(\frac{1}{3} + (f_{\mathbf{k}} - 1)\sin^2\theta_{\mathbf{k}}\right), \tag{2.5.7b}$$

$$D_{\mathbf{k}}^{zz} = \frac{4\pi\mu^2}{a^3}\left(\frac{1}{3} + (f_{\mathbf{k}} - 1)\cos^2\theta_{\mathbf{k}}\right), \tag{2.5.7c}$$

$$D_{\mathbf{k}}^{xy} = 0, \tag{2.5.7d}$$

$$D_{\mathbf{k}}^{xz} = 0, \tag{2.5.7e}$$

$$D_{\mathbf{k}}^{yz} = \frac{2\pi\mu^2}{a^3}(f_{\mathbf{k}} - 1)\sin(2\theta_{\mathbf{k}}). \tag{2.5.7f}$$

In the above expression we introduced the form factor

$$f_{\mathbf{k}} = \frac{1 - e^{-|\mathbf{k}|d}}{|\mathbf{k}|d}, \tag{2.5.8}$$

which up to first order in $|\mathbf{k}|d$ equals $e^{-\frac{|\mathbf{k}|d}{2}} = 1 - \frac{|\mathbf{k}|d}{2} + \mathcal{O}(|\mathbf{k}|^2 d^2)$. From now on we will use the form factor from eqn. (2.5.8), because it has been shown in previous results [14] that it provides a more accurate approximation to numerical results than the uniform mode approximation does. By combining eqn. (2.4.4) with eqn. (2.5.1) and eqn. (2.5.7) we obtain an explicit form of $A_{\mathbf{k}}$ and $B_{\mathbf{k}}$ that we can write as

$$A_{\mathbf{k}} = B + 2JS\left(2 - \cos(k_y a) - \cos(k_z a)\right) - \frac{S}{2}\left(D_{\mathbf{k}}^{xx} + D_{\mathbf{k}}^{yy}\right) + S\frac{4\pi\mu^2}{3a^3}, \tag{2.5.9a}$$

$$B_{\mathbf{k}} = -\frac{S}{2}\left(D_{\mathbf{k}}^{xx} - D_{\mathbf{k}}^{yy}\right). \tag{2.5.9b}$$

2.6 Magnon-magnon interactions

2.6.1 Three-magnon interactions

We perform a Fourier transformation of the cubic term of the Hamiltonian, that is given in eqn. (2.3.5), to obtain H_3 as

$$H_3 = \sqrt{\frac{S}{2N}} \sum_{\mathbf{k}_1,\mathbf{k}_2,\mathbf{k}_3} \Bigg[\delta_{\mathbf{k}_1+\mathbf{k}_2+\mathbf{k}_3,0} \times \left\{ \left(D^{xz}_{\mathbf{k}_2} + iD^{yz}_{\mathbf{k}_2} + \frac{1}{4}D^{xz}_{0} + \frac{i}{4}D^{yz}_{0} \right) b^{\dagger}_{\mathbf{k}_1} b^{\dagger}_{\mathbf{k}_2} b_{-\mathbf{k}_3} + h.c. \right\} \Bigg]. \tag{2.6.1}$$

For the sake of simplicity we rewrite eqn. (2.6.1) as

$$H_3 = \frac{1}{\sqrt{N}} \sum_{\mathbf{k}_1,\mathbf{k}_2,\mathbf{k}_3} \left[\delta_{\mathbf{k}_1+\mathbf{k}_2+\mathbf{k}_3,0} \left(\frac{1}{2}\Gamma^{\bar{b}bb}_{1;23} b^{\dagger}_1 b_{-2} b_{-3} + \frac{1}{2}\Gamma^{\bar{b}\bar{b}b}_{12;3} b^{\dagger}_1 b^{\dagger}_2 b_{-3} \right) \right], \tag{2.6.2}$$

where the sub-index i corresponds to $\mathbf{k}_i$ and $-i$ corresponds to $-\mathbf{k}_i$, and with

$$\Gamma^{\bar{b}\bar{b}b}_{pq;r} = \sqrt{\frac{S}{2}} \left[D^{xz}_{\mathbf{k}_p} + iD^{yz}_{\mathbf{k}_p} + (\mathbf{k}_p \to \mathbf{k}_q) + \frac{1}{2}D^{xz}_{0} + \frac{i}{2}D^{yz}_{0} \right], \tag{2.6.3a}$$

$$\Gamma^{\bar{b}bb}_{p;qr} = \left(\Gamma^{\bar{b}\bar{b}b}_{rq;p} \right)^{*}. \tag{2.6.3b}$$

By plugging the Bogoliubov transformation given in eqn. (2.4.6) into eqn. (2.6.2) we obtain

$$H_3 = \frac{1}{\sqrt{N}} \sum_{\mathbf{k}_1,\mathbf{k}_2,\mathbf{k}_3} \Bigg[\delta_{\mathbf{k}_1+\mathbf{k}_2+\mathbf{k}_3,0} \Bigg(\frac{1}{3!}\Gamma^{aaa}_{123} a_{-1} a_{-2} a_{-3} + \frac{1}{2}\Gamma^{\bar{a}aa}_{1;23} a^{\dagger}_1 a_{-2} a_{-3} + \frac{1}{2}\Gamma^{\bar{a}\bar{a}a}_{12;3} a^{\dagger}_1 a^{\dagger}_2 a_{-3} + \frac{1}{3!}\Gamma^{\bar{a}\bar{a}\bar{a}}_{123} a^{\dagger}_1 a^{\dagger}_2 a^{\dagger}_3 \Bigg) \Bigg], \tag{2.6.4}$$

with

$$\begin{aligned}
\Gamma^{aaa}_{123} =& v_1 v_2 u_3 \Gamma^{\bar{b}\bar{b}b}_{12;3} + v_1 v_3 u_2 \Gamma^{\bar{b}\bar{b}b}_{13;2} + v_2 v_3 u_1 \Gamma^{\bar{b}\bar{b}b}_{23;1} \\
& - v_1 u_2 u_3 \Gamma^{\bar{b}bb}_{1;23} - v_2 u_1 u_3 \Gamma^{\bar{b}bb}_{2;13} - v_3 u_1 u_2 \Gamma^{\bar{b}bb}_{3;12}, && \text{(2.6.5a)} \\
\Gamma^{\bar{a}aa}_{1;23} =& - u_1 v_2 u_3 \Gamma^{\bar{b}\bar{b}b}_{12;3} - u_1 u_2 v_3 \Gamma^{\bar{b}\bar{b}b}_{13;2} - v_1 v_2 v_3 \Gamma^{\bar{b}\bar{b}b}_{23;1} \\
& + u_1 u_2 u_3 \Gamma^{\bar{b}bb}_{1;23} + v_1 v_2 u_3 \Gamma^{\bar{b}bb}_{2;13} + v_1 u_2 v_3 \Gamma^{\bar{b}bb}_{3;12}, && \text{(2.6.5b)} \\
\Gamma^{\bar{a}\bar{a}a}_{12;3} =& \left(\Gamma^{\bar{a}aa}_{3;12} \right)^{*}, && \text{(2.6.5c)} \\
\Gamma^{\bar{a}\bar{a}\bar{a}}_{123} =& \left(\Gamma^{aaa}_{123} \right)^{*}. && \text{(2.6.5d)}
\end{aligned}$$

2.6.2 Four-magnon interactions

Let us perform a Fourier transformation of the quartic term of the Hamiltonian, which is given in eqn. (2.3.6), to rewrite H_4 as

$$H_4 = -\frac{1}{2N}\sum_{\mathbf{k}_1,\mathbf{k}_2,\mathbf{k}_3,\mathbf{k}_4}\Bigg[\delta_{\mathbf{k}_1+\mathbf{k}_2+\mathbf{k}_3+\mathbf{k}_4,0}\Bigg\{\Bigg(J_{\mathbf{k}_2+\mathbf{k}_3}+D^{zz}_{\mathbf{k}_2+\mathbf{k}_3}-\frac{1}{2}J_{\mathbf{k}_2}-\frac{1}{2}J_{\mathbf{k}_4} \\ -\frac{1}{4}D^{xx}_{\mathbf{k}_2}-\frac{1}{4}D^{yy}_{\mathbf{k}_2}-\frac{1}{4}D^{xx}_{\mathbf{k}_4}-\frac{1}{4}D^{yy}_{\mathbf{k}_4}\Bigg)b^\dagger_{\mathbf{k}_1}b^\dagger_{\mathbf{k}_2}b_{-\mathbf{k}_3}b_{-\mathbf{k}_4} \\ -\frac{1}{4}\left[\left(D^{xx}_{\mathbf{k}_2}+2iD^{xy}_{\mathbf{k}_2}-D^{yy}_{\mathbf{k}_2}\right)b^\dagger_{\mathbf{k}_1}b^\dagger_{\mathbf{k}_2}b^\dagger_{\mathbf{k}_3}b_{-\mathbf{k}_4}+h.c.\right]\Bigg\}\Bigg]. \tag{2.6.6}$$

For the sake of simplicity we rewrite eqn. (2.6.6) as

$$H_4 = \frac{1}{N}\sum_{\mathbf{k}_1,\mathbf{k}_2,\mathbf{k}_3,\mathbf{k}_4}\Bigg[\delta_{\mathbf{k}_1+\mathbf{k}_2+\mathbf{k}_3+\mathbf{k}_4,0}\Bigg(\frac{1}{(2!)^2}\Gamma^{\bar{b}\bar{b}bb}_{12;34}b^\dagger_1b^\dagger_2b_{-3}b_{-4} \\ +\frac{1}{3!}\Gamma^{\bar{b}\bar{b}\bar{b}b}_{123;4}b^\dagger_1b^\dagger_2b^\dagger_3b_{-4}+\frac{1}{3!}\Gamma^{\bar{b}bbb}_{1;234}b^\dagger_1b_{-2}b_{-3}b_{-4}\Bigg)\Bigg], \tag{2.6.7}$$

with

$$\Gamma^{\bar{b}\bar{b}bb}_{pq;rs} = -\frac{1}{2}\Bigg(J_{\mathbf{k}_p+\mathbf{k}_r}+J_{\mathbf{k}_p+\mathbf{k}_s}+J_{\mathbf{k}_q+\mathbf{k}_r}+J_{\mathbf{k}_q+\mathbf{k}_s}+D^{zz}_{\mathbf{k}_p+\mathbf{k}_r} \\ +D^{zz}_{\mathbf{k}_p+\mathbf{k}_s}+D^{zz}_{\mathbf{k}_q+\mathbf{k}_r}+D^{zz}_{\mathbf{k}_q+\mathbf{k}_s}-\sum_{i=1}^{4}\left(J_{\mathbf{k}_i}+\frac{1}{2}D^{xx}_{\mathbf{k}_i}+\frac{1}{2}D^{yy}_{\mathbf{k}_i}\right)\Bigg), \tag{2.6.8}$$

$$\Gamma^{\bar{b}\bar{b}\bar{b}b}_{pqr;s} = \frac{1}{4}\left(\ D^{xx}_{\mathbf{k}_p}+2iD^{xy}_{\mathbf{k}_p}-D^{yy}_{\mathbf{k}_p}+(\mathbf{k}_p\to\mathbf{k}_q)+(\mathbf{k}_p\to\mathbf{k}_r)\right), \tag{2.6.9}$$

$$\Gamma^{\bar{b}bbb}_{p;qrs} = \left(\ \Gamma^{\bar{b}\bar{b}\bar{b}b}_{qrs;p}\right)^*. \tag{2.6.10}$$

By plugging eqn. (2.4.6) into eqn. (2.6.7) we obtain H_4 as

$$H_4 = \frac{1}{N}\sum_{\mathbf{k}_1,\mathbf{k}_2,\mathbf{k}_3,\mathbf{k}_4}\Bigg[\delta_{\mathbf{k}_1+\mathbf{k}_2+\mathbf{k}_3+\mathbf{k}_4,0}\Bigg(\frac{1}{4!}\Gamma^{aaaa}_{1234}a_{-1}a_{-2}a_{-3}a_{-4} \\ +\frac{1}{3!}\Gamma^{\bar{a}aaa}_{1;234}a^\dagger_1a_{-2}a_{-3}a_{-4}+\frac{1}{(2!)^2}\Gamma^{\bar{a}\bar{a}aa}_{12;34}a^\dagger_1a^\dagger_2a_{-3}a_{-4} \tag{2.6.11}$$

$$+\frac{1}{3!}\Gamma^{\bar{a}\bar{a}\bar{a}a}_{123;4}a^\dagger_1a^\dagger_2a^\dagger_3a_{-4}+\frac{1}{4!}\Gamma^{\bar{a}\bar{a}\bar{a}\bar{a}}_{1234}a^\dagger_1a^\dagger_2a^\dagger_3a^\dagger_4\Bigg)\Bigg], \tag{2.6.12}$$

with

$$\begin{aligned}
\Gamma^{aaaa}_{1234} =& v_1v_2u_3u_4\Gamma^{\bar{b}\bar{b}bb}_{12;34} + v_1v_3u_2u_4\Gamma^{\bar{b}\bar{b}bb}_{13;24} + v_1v_4u_2u_3\Gamma^{\bar{b}\bar{b}bb}_{14;23} \\
&+ v_3v_4u_1u_2\Gamma^{\bar{b}\bar{b}bb}_{34;12} + v_2v_4u_1u_3\Gamma^{\bar{b}\bar{b}bb}_{24;13} + v_2v_3u_1u_4\Gamma^{\bar{b}\bar{b}bb}_{23;14} \\
&- v_1v_2v_3u_4\Gamma^{\bar{b}\bar{b}\bar{b}b}_{123;4} - v_1v_2v_4u_3\Gamma^{\bar{b}\bar{b}\bar{b}b}_{124;3} - v_1v_3v_4u_2\Gamma^{\bar{b}\bar{b}\bar{b}b}_{134;2} \\
&- v_2v_3v_4u_1\Gamma^{\bar{b}\bar{b}\bar{b}b}_{234;1} - v_1u_2u_3u_4\Gamma^{\bar{b}bbb}_{1;234} - v_2u_1u_3u_4\Gamma^{\bar{b}bbb}_{2;134} \\
&- v_3u_1u_2u_4\Gamma^{\bar{b}bbb}_{3;124} - v_4u_1u_2u_3\Gamma^{\bar{b}bbb}_{4;123}, \qquad (2.6.13a) \\
\Gamma^{\bar{a}aaa}_{1;234} =& - u_1v_2u_3u_4\Gamma^{\bar{b}\bar{b}bb}_{12;34} - u_1u_2v_3u_4\Gamma^{\bar{b}\bar{b}bb}_{13;24} - u_1u_2u_3v_4\Gamma^{\bar{b}\bar{b}bb}_{14;23} \\
&- v_1v_2v_3u_4\Gamma^{\bar{b}\bar{b}bb}_{23;14} - v_1v_2u_3v_4\Gamma^{\bar{b}\bar{b}bb}_{24;31} - v_1u_2v_3v_4\Gamma^{\bar{b}\bar{b}bb}_{34;12} \\
&+ v_1v_2v_3v_4\Gamma^{\bar{b}\bar{b}\bar{b}b}_{234;1} + u_1u_2v_3v_4\Gamma^{\bar{b}\bar{b}\bar{b}b}_{134;2} + u_1v_2u_3v_4\Gamma^{\bar{b}\bar{b}\bar{b}b}_{124;3} \\
&+ u_1v_2v_3u_4\Gamma^{\bar{b}\bar{b}\bar{b}b}_{123;4} + u_1u_2u_3u_4\Gamma^{\bar{b}bbb}_{1;234} + v_1v_2u_3u_4\Gamma^{\bar{b}bbb}_{2;134} \\
&+ v_1u_2v_3u_4\Gamma^{\bar{b}bbb}_{3;124} + v_1u_2u_3v_4\Gamma^{\bar{b}bbb}_{4;123}, \qquad (2.6.13b) \\
\Gamma^{\bar{a}\bar{a}aa}_{12;34} =& u_1u_2u_3u_4\Gamma^{\bar{b}\bar{b}bb}_{12;34} + u_1v_2v_3u_4\Gamma^{\bar{b}\bar{b}bb}_{13;24} + u_1v_2u_3v_4\Gamma^{\bar{b}\bar{b}bb}_{14;23} \\
&+ v_1u_2v_3u_4\Gamma^{\bar{b}\bar{b}bb}_{23;14} + v_1u_2u_3v_4\Gamma^{\bar{b}\bar{b}bb}_{24;13} + v_1u_2v_3v_4^*\Gamma^{\bar{b}\bar{b}bb}_{34;12} \\
&- u_1u_2v_3u_4\Gamma^{\bar{b}\bar{b}\bar{b}b}_{123;4} - u_1u_2u_3v_4\Gamma^{\bar{b}\bar{b}\bar{b}b}_{124;3} - u_1v_2v_3v_4\Gamma^{\bar{b}\bar{b}\bar{b}b}_{134;2} \\
&- v_1u_2v_3v_4\Gamma^{\bar{b}\bar{b}\bar{b}b}_{234;1} - u_1v_2u_3u_4\Gamma^{\bar{b}bbb}_{1;234} - v_1u_2u_3u_4\Gamma^{\bar{b}bbb}_{2;134} \\
&- v_1v_2v_3u_4\Gamma^{\bar{b}bbb}_{3;124} - v_1v_2u_3v_4\Gamma^{\bar{b}bbb}_{4;123}, \qquad (2.6.13c) \\
\Gamma^{\bar{a}\bar{a}\bar{a}a}_{123;4} =& \left(\Gamma^{\bar{a}aaa}_{4;123}\right)^*, \qquad (2.6.13d) \\
\Gamma^{\bar{a}\bar{a}\bar{a}\bar{a}}_{1234} =& \left(\Gamma^{aaaa}_{1234}\right)^*. \qquad (2.6.13e)
\end{aligned}$$

The main results of this chapter are the non-interacting magnon dispersion relation in eqn. (2.4.11), and the four-magnon interactions in eqn. (2.6.13c). In the next chapter we will use these results to determine the stability of the magnon condensate.

Chapter 3

Critical density

In this chapter we provide results obtained from applying the theoretical model described in Chapter 2 to a thin film of YIG in an external magnetic field. In the last part of this chapter we obtain a critical density of magnons in a BEC in a way similar to Ref. [8].

3.1 Dispersion of the lowest magnon band

We have found that the dispersion of the lowest magnon band is given by eqn. (2.4.11). In Fig. 3.1 a graph of the spectrum is depicted. We have chosen to consider an external magnetic field $H_e = 700$ G and a film thickness $d = 5\,\mu$m, because for this field strength and film thickness the dispersion shows the features that are relevant for this research and these values are used in experiments [6]. We have numerically calculated that for this field strength the minimum of the dispersion occurs at the wave-vector

$$k_0 = 5.5\,\mu\text{m}^{-1}. \tag{3.1.1}$$

We have calculated the value of the wave-vector at the minimum of the dispersion as a function of the external magnetic field. The result obtained is depicted in Fig. 3.2. This figure shows that the value of the wave-vector at the the minimum of the dispersion increases, but decreasingly fast, as the strength of the external magnetic field increases.

3.2 Attractive interaction in BEC

We are interested in the behavior of the interactions in the BEC in order to investigate the stability of the BEC. We plotted the vertex, $\Gamma = \Gamma^{\bar{a}\bar{a}aa}_{k_0 k_0; -k_0 - k_0}$

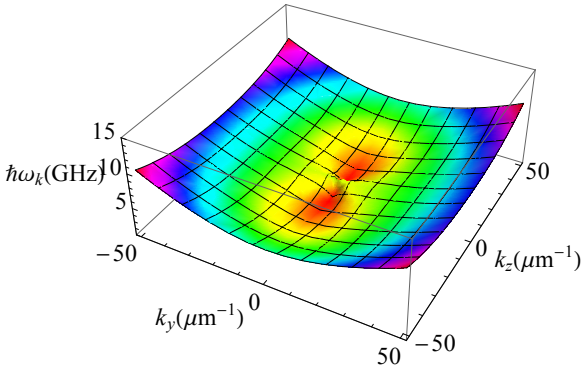

(a) For the y- and z-direction.

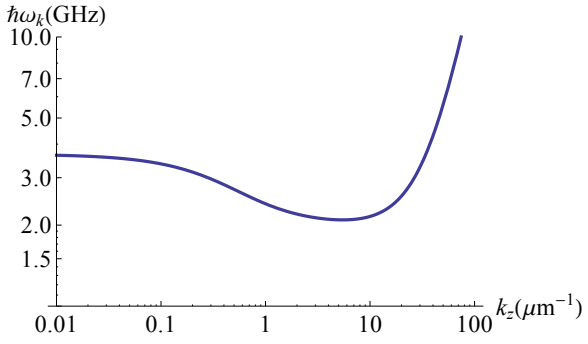

(b) $k_y = 0$.

Figure 3.1: The dispersion of the lowest magnon band with $H_e = 700$ G and $d = 5\,\mu$m.

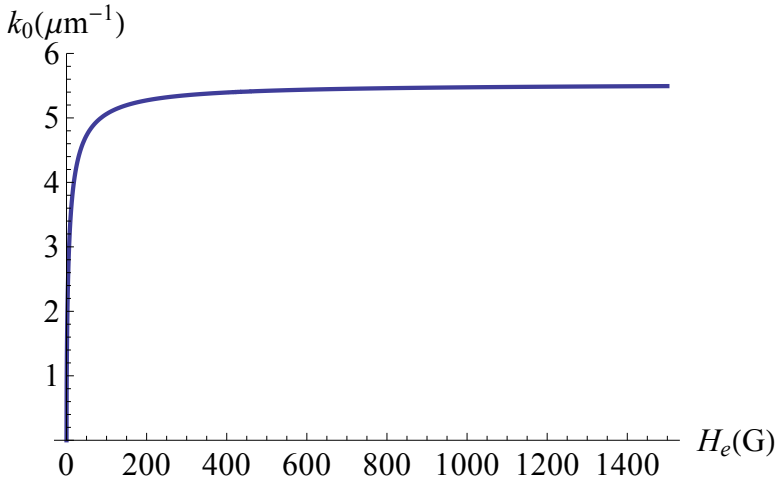

Figure 3.2: The value of the wave-vector at the minimum of the dispersion as a function of the external magnetic field.

given in eqn. (2.6.13c) evaluated at the minimum of the dispersion as a function of the external magnetic field in Fig. 3.3.

From Fig. 3.3 we can read off that this vertex is negative in the for experimentally relevant magnetic field strengths, because usually field strengths between $600 - 800$ G are being used. This indicates that the interaction is attractive, because the energy decreases if the density increases, hence it is possible that the condensate becomes in-stable and collapses in the situation where this term is dominant in the interaction, for example when only one valley of the dispersion is occupied.

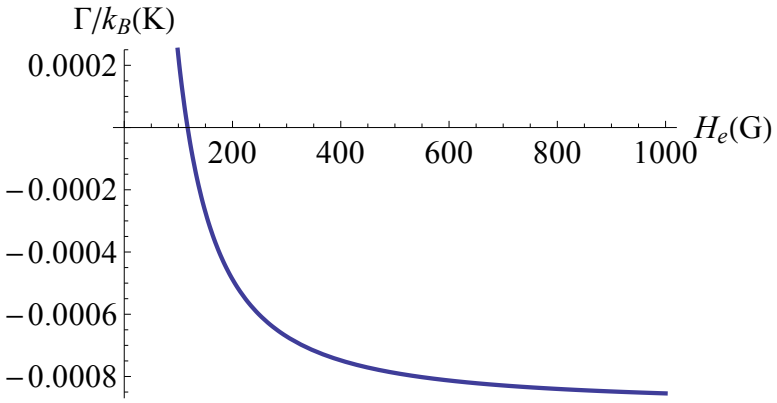

Figure 3.3: The vertex, Γ, evaluated at the minimum of the dispersion as a function of the external magnetic field. Here, k_{B} is the Boltzmann constant.

3.3 Critical density

In order to estimate at what value the density becomes critical, i.e. when the BEC will collapse, we focus on the term for the interaction within one valley of which we know it can be negative and introduce the zero-point energy

$$\hbar\omega_{\mathrm{zp}} = \hbar\omega_{k_0+\frac{\pi}{L}} - \hbar\omega_{k_0}, \tag{3.3.1}$$

with L the length of the film in the direction of the wave. The zero-point energy is the minimum of energy that is present in finite systems due to the zero-point motion resulting from the confinement. We estimate the critical density by calculating when the interaction energy is of the same order as the zero-point energy. This is the density at which the self-attraction overcomes the stabilizing zero-point motion. The critical density is then given as

$$n_{\mathrm{crit}} = \frac{\hbar\omega_{\mathrm{zp}}}{|\Gamma|}. \tag{3.3.2}$$

In the experiment [6] the size of the film is $20 \times 2\,\mathrm{mm}^2$. We then find as estimate for the critical densities in the order of magnitude of 10^{-8} and 10^{-6}, expressed in magnons per site, for waves in respectively the direction of the long side and the short side of the film. This result is in good correspondence with [8]. To convert this to a density with the correct dimensions we divide by a^2 and obtain densities of respectively $10^5\,\mathrm{cm}^{-2}$ and $10^7\,\mathrm{cm}^{-2}$.

Chapter 4

Dynamics in the BEC state

The goal of this chapter is to describe the dynamics in the BEC state. To get a first insight into the dynamics we perform a stability analysis in the static BEC ansatz. Next we introduce the Gaussian ansatz and again perform a static stability analysis. And then we derive equations of motion and study the influence of the Gilbert damping and the parametric pumping on the stability of the BEC.

4.1 Energy functional

Let us begin by rewriting the magnon Hamiltonian obtained in Chapter 2 into an energy functional. First rewrite the kinetic part of the second order term as given in eqn. (2.4.13) as

$$\sum_{\mathbf{k}} \hbar\omega_{\mathbf{k}} a^{\dagger}_{\mathbf{k}} a_{\mathbf{k}} = \int \mathrm{d}\vec{x}\, (\Phi_1^* \hbar\omega(\partial_{\vec{x}})\Phi_1 + \Phi_2^* \hbar\omega(\partial_{\vec{x}})\Phi_2)\,, \tag{4.1.1}$$

where $\hbar\omega(\partial_{\vec{x}}) = \hbar\omega_{\vec{k}_0} - \frac{\hbar^2\partial_{x_1}^2}{2m_{x_1}} - \frac{\hbar^2\partial_{x_2}^2}{2m_{x_2}}$ and with Φ_1 and Φ_2 corresponding to the field at respectively $\mathbf{k}_0$ and $-\mathbf{k}_0$. m_{x_1} and m_{x_2} are effective masses that can be determined by Taylor expanding the dispersion relation around $\mathbf{k}_0$ up to second order in $\mathbf{k}$, hence we approximate the behavior of the dispersion relation near the minimum with a parabola.

We introduce a pumping term

$$\sum_{\mathbf{k}} \left[\frac{\boldsymbol{\nu}^*_{\mathbf{k}}}{2} a^{\dagger}_{\mathbf{k}} a^{\dagger}_{-\mathbf{k}} + \frac{\boldsymbol{\nu}_{\mathbf{k}}}{2} a_{\mathbf{k}} a_{-\mathbf{k}} \right], \tag{4.1.2}$$

with $\boldsymbol{\nu}_{\mathbf{k}}$ the pumping frequency, to the magnon Hamiltonian in order to model the influence of the pumping as described in [6, 11]. Rewrite this pumping

term as

$$\sum_{\mathbf{k}} \left[\frac{\boldsymbol{\nu}_{\mathbf{k}}^*}{2} a_{\mathbf{k}}^\dagger a_{-\mathbf{k}}^\dagger + \frac{\boldsymbol{\nu}_{\mathbf{k}}}{2} a_{\mathbf{k}} a_{-\mathbf{k}} \right] = \int \mathrm{d}\vec{x} \left(\boldsymbol{\nu}^* \Phi_1^* \Phi_2^* + \boldsymbol{\nu} \Phi_1 \Phi_2 \right), \tag{4.1.3}$$

with

$$\boldsymbol{\nu} = \boldsymbol{\nu}_{\mathbf{k}_0} + \boldsymbol{\nu}_{-\mathbf{k}_0}. \tag{4.1.4}$$

At low energies the confluence and splitting terms are negligible, thus third order terms drop and of the fourth order terms only the two-magnon scattering term remains. Rewrite the two-magnon scattering term as

$$\begin{aligned}
&\frac{1}{2N} \sum_{\mathbf{k}_1,\mathbf{k}_2,\mathbf{k}_3,\mathbf{k}_4} \delta_{\mathbf{k}_1+\mathbf{k}_2+\mathbf{k}_3+\mathbf{k}+4,0} \Gamma^{\bar{a}\bar{a}aa}_{\mathbf{k}_1\mathbf{k}_2;\mathbf{k}_3\mathbf{k}_4} a^\dagger_{\mathbf{k}_1} a^\dagger_{\mathbf{k}_2} a_{-\mathbf{k}_3} a_{-\mathbf{k}_4} = \\
&\frac{1}{2N} \sum_{\mathbf{p}_1,\mathbf{p}_2,\mathbf{p}_3,\mathbf{p}_4} \delta_{\mathbf{p}_1+\mathbf{p}_2+\mathbf{p}_3+\mathbf{p}_4,0} \Bigg[4\Gamma^{\bar{a}\bar{a}aa}_{\mathbf{k}_0-\mathbf{k}_0;\mathbf{k}_0-\mathbf{k}_0} a^\dagger_{\mathbf{k}_0+\mathbf{p}_1} a^\dagger_{-\mathbf{k}_0+\mathbf{p}_2} a_{\mathbf{k}_0-\mathbf{p}_3} a_{-\mathbf{k}_0-\mathbf{p}_4} \\
&+ \Gamma^{\bar{a}\bar{a}aa}_{\mathbf{k}_0\mathbf{k}_0;-\mathbf{k}_0-\mathbf{k}_0} \left(a^\dagger_{-\mathbf{k}_0+\mathbf{p}_1} a^\dagger_{-\mathbf{k}_0+\mathbf{p}_2} a_{-\mathbf{k}_0-\mathbf{p}_3} a_{-\mathbf{k}_0-\mathbf{p}_4} + a^\dagger_{\mathbf{k}_0+\mathbf{p}_1} a^\dagger_{\mathbf{k}_0+\mathbf{p}_2} a_{\mathbf{k}_0-\mathbf{p}_3} a_{\mathbf{k}_0-\mathbf{p}_4} \right) \Bigg].
\end{aligned} \tag{4.1.5}$$

By performing an inverse Fourier transform, carrying out the momentum sums and integrating over the resulting Dirac delta functions we obtain

$$\int \mathrm{d}\vec{x} \left[2\Gamma^{\bar{a}\bar{a}aa}_{\mathbf{k}_0-\mathbf{k}_0;\mathbf{k}_0-\mathbf{k}_0} \Phi_1^* \Phi_1 \Phi_2^* \Phi_2 + \frac{1}{2} \Gamma^{\bar{a}\bar{a}aa}_{\mathbf{k}_0\mathbf{k}_0;-\mathbf{k}_0-\mathbf{k}_0} \left(\Phi_1^* \Phi_1 \Phi_1^* \Phi_1 + \Phi_2^* \Phi_2 \Phi_2^* \Phi_2 \right) \right], \tag{4.1.6}$$

which we rewrite as

$$\int \mathrm{d}\vec{x} \left[\frac{\gamma_1}{2} \left(\Phi_1^* \Phi_1 + \Phi_2^* \Phi_2 \right)^2 + \frac{\gamma_2}{2} \left(\Phi_1^* \Phi_1 - \Phi_2^* \Phi_2 \right)^2 \right] \tag{4.1.7}$$

with

$$\gamma_1 + \gamma_2 = \Gamma^{\bar{a}\bar{a}aa}_{\mathbf{k}_0\mathbf{k}_0;-\mathbf{k}_0-\mathbf{k}_0}, \qquad \gamma_1 - \gamma_2 = 2\Gamma^{\bar{a}\bar{a}aa}_{\mathbf{k}_0-\mathbf{k}_0;\mathbf{k}_0-\mathbf{k}_0} \tag{4.1.8}$$

By combining the derived terms of the Hamiltonian and adding a chemical potential we obtain the energy functional as in [15],

$$\begin{aligned}
\epsilon\left[\Phi, \Phi^*\right] = \int \mathrm{d}\mathbf{r} \Bigg(&\Phi_1^* \hbar\omega(\partial_{\vec{x}}) \Phi_1 + \Phi_2^* \hbar\omega(\partial_{\vec{x}}) \Phi_2 - \mu \left(\Phi_1^* \Phi_1 + \Phi_2^* \Phi_2 \right) \\
&+ \boldsymbol{\nu} \Phi_1 \Phi_2 + \boldsymbol{\nu}^* \Phi_1^* \Phi_2^* + \frac{\gamma_1}{2} \left(\Phi_1^* \Phi_1 + \Phi_2^* \Phi_2 \right)^2 + \frac{\gamma_2}{2} \left(\Phi_1^* \Phi_1 - \Phi_2^* \Phi_2 \right)^2 \Bigg).
\end{aligned} \tag{4.1.9}$$

Interesting to note is that $U(1)$-symmetry

$$\Phi_1 \to \mathrm{e}^{i\delta}\Phi_1, \qquad \Phi_2 \to \mathrm{e}^{i\delta}\Phi_2, \tag{4.1.10}$$

and likewise the conjugates undergo the inverse transformation, associated with particle number conservation is broken by the magnon pumping terms. Also the interactions that are third order in the magnon operators do not preserve the number of magnons, but since we focus on interactions between condensed magnons the third order interactions do not play a role here. Despite the $U(1)$-symmetry breakdown the energy functional is still invariant under the transformation

$$\Phi_1 \to \mathrm{e}^{i\delta}\Phi_1, \qquad \Phi_2 \to \mathrm{e}^{-i\delta}\Phi_2. \tag{4.1.11}$$

4.2 Static and homogeneous BEC

By inserting the static Bose-Einstein condensate ansatz $\Phi_i = \sqrt{n_i}e^{i\theta_i}$, with n_i the density and θ_i the phase factor, into eqn. (4.1.9) we obtain

$$\begin{aligned}\frac{\epsilon}{A} = (\hbar\omega_{k_0} - \mu)(n_1 + n_2) + 2\nu\sqrt{n_1 n_2}\cos(\theta_1 + \theta_2 + \theta_\nu) \\ + \frac{\gamma_1}{2}(n_1 + n_2)^2 + \frac{\gamma_2}{2}(n_1 - n_2)^2,\end{aligned} \tag{4.2.1}$$

where we have rewritten $\boldsymbol{\nu} = \nu e^{i\theta_\nu}$. We perform a change of variables as

$$n_1 = \frac{n+m}{2}, \qquad n_2 = \frac{n-m}{2}, \tag{4.2.2}$$

such that n corresponds to the total density and that m corresponds to the difference in densities between the two minima. Combining eqn. (4.2.2) and eqn. (4.2.1) yields

$$\frac{\epsilon}{A} = n(\hbar\omega_{k_0} - \mu) + \nu\sqrt{n^2 - m^2}\cos(\theta_{\mathrm{tot}} + \theta_\nu) + \frac{\gamma_1}{2}n^2 + \frac{\gamma_2}{2}m^2, \tag{4.2.3}$$

with $\theta_{\mathrm{tot}} = \theta_1 + \theta_2$. Let us consider ϵ as $\epsilon(n, m, \theta_{\mathrm{tot}})$ where $0 \leq n < \infty, -n \leq m \leq n$ and $0 \leq \theta_{\mathrm{tot}} < 2\pi$. We are interested in what the conditions on $\mu, \nu, \theta_\nu, \gamma_1$ and γ_2 are such that $\epsilon(n, m, \theta_{\mathrm{tot}})$ has a local minimum. From eqn. (4.2.3) we obtain that minimizing $\epsilon(n, m, \theta_{\mathrm{tot}})$ with respect to θ_{tot} yields that $\theta_{\mathrm{tot}} = (2k+1)\pi - \theta_\nu$ with $k \in \{0, 1\}$. By plugging this value for θ_{tot} into $\epsilon(n, m, \theta_{\mathrm{tot}})$ allows us to reduce the possible solutions for stable minima of $\epsilon(n, m, \theta_{\mathrm{tot}})$, hence we can restrict ourselves to minimizing $\epsilon(n, m, (2k+1)\pi - \theta_\nu)$ with respect to n and m.

In order for a point to be a stable minimum, it must be a stationary point. The stationary points of $\epsilon(n, m, (2k+1)\pi - \theta_\nu)$ have to obey

$$\frac{\partial \epsilon}{\partial n} = \hbar\omega_{k_0} - \mu - \frac{n\nu}{\sqrt{n^2 - m^2}} + \gamma_1 n = 0, \tag{4.2.4a}$$

$$\frac{\partial \epsilon}{\partial m} = m\left(\frac{\nu}{\sqrt{n^2 - m^2}} + \gamma_2\right) = 0. \tag{4.2.4b}$$

We find two types of solutions. The first is

$$(n, m, \theta_{\text{tot}}) = \left(\frac{-\hbar\omega_{k_0} + \mu + \nu}{\gamma_1}, 0, (2k+1)\pi - \theta_\nu\right), \tag{4.2.5}$$

under the condition that $\frac{-\hbar\omega_{k_0}+\mu+\nu}{\gamma_1} > 0$, and the second

$$(n, m, \theta_{\text{tot}}) = \left(-\frac{\hbar\omega_{k_0} - \mu}{\gamma_1 + \gamma_2}, \pm\sqrt{\left(\frac{\hbar\omega_{k_0} - \mu}{\gamma_1 + \gamma_2}\right)^2 - \left(\frac{\nu}{\gamma_2}\right)^2}, (2k+1)\pi - \theta_\nu\right), \tag{4.2.6}$$

with $k \in \{0, 1\}$ and under the conditions that $-\frac{\hbar\omega_{k_0}-\mu}{\gamma_1+\gamma_2} > \frac{\nu}{|\gamma_2|}$ and $\gamma_2 < 0$.

The conditions under which these stationary points are local minima are given by

$$\frac{\partial^2 \epsilon}{\partial n^2} = \frac{m^2\nu}{(n^2 - m^2)^{\frac{3}{2}}} + \gamma_1 > 0, \tag{4.2.7a}$$

$$\frac{\partial^2 \epsilon}{\partial m^2} = \frac{n^2\nu}{(n^2 - m^2)^{\frac{3}{2}}} + \gamma_2 > 0, \tag{4.2.7b}$$

$$\frac{\partial^2 \epsilon}{\partial n^2}\frac{\partial^2 \epsilon}{\partial m^2} - \left(\frac{\partial^2 \epsilon}{\partial n \partial m}\right)^2 = \frac{\nu\left(\gamma_1 n^2 + \gamma_2 m^2\right)}{(n^2 - m^2)^{\frac{3}{2}}} + \gamma_1\gamma_2 > 0. \tag{4.2.7c}$$

By inserting the stationary point given in eqn. (4.2.5) into the conditions given in eqn. (4.2.7) we obtain that in order for the stationary point from eqn. (4.2.5) to be a local minimum

$$\gamma_1 > 0, \qquad \gamma_2 > -\frac{\nu}{n}, \tag{4.2.8}$$

where we have written n for $\frac{-\hbar\omega_{k_0}+\mu+\nu}{\gamma_1}$. By plugging the stationary point given in eqn. (4.2.6) into the conditions given in eqn. (4.2.7) we obtain that in order for the stationary point from eqn. (4.2.6) to be a local minimum

$$\gamma_1 > |\gamma_2|, \qquad \gamma_2 < -\frac{\nu}{n}, \tag{4.2.9}$$

where we have written n for $-\frac{\hbar\omega_{k_0}-\mu}{\gamma_1+\gamma_2}$.

Let us consider if there is a stable minimum at a boundary of $\epsilon(n, m, (2k+1)\pi-\theta_\nu)$, hence for $m = \pm n$. We are not interested in the case $n = 0$, because there will not be any dynamics. From the expression for $\frac{\partial\epsilon}{\partial m}$ given in eqn. (4.2.4) we read off that there is no local minimum for $m = \pm n$, because $\frac{\partial\epsilon}{\partial m} \to \pm\infty$ if $m \to \pm n$.

Note however that when $\nu = 0$, i.e. when there is no pumping, then the solution in eqn. (4.2.6) states $n = m$, thus only one valley is occupied.

In summary, we found that there are two different types of static solutions, one symmetric and the other asymmetric, that can both be stable. The value of the pumping is important for the question whether or not the condensates are stable as follows from the conditions for the symmetric condensate in eqn. (4.2.8) and for the asymmetric condensate in eqn. (4.2.9).

4.3 Gaussian ansatz

We introduce a Gaussian ansatz in order to take dynamics of the BEC into account. By using a Gaussian ansatz of the form [9]

$$\Phi_i(\vec{x},t) \propto \sqrt{N_i(t)} \prod_{j=1,2} \exp\left(-\frac{x_j^2}{2q_{i,x_j}^2(t)}\left(1 - i\frac{m_{x_j} q_{i,x_j}(t)}{\hbar}\frac{\mathrm{d}q_{i,x_j}}{\mathrm{d}t}\right) + \frac{i}{2}\theta_i(t)\right), \tag{4.3.1}$$

with N_i the number of magnons in valley i, q_{i,x_j} the Gaussian width of valley i in the direction x_j and θ_i the phase factor of valley i, in the normalization requirement

$$\int \mathrm{d}^2x |\Phi_i(\vec{x},t)|^2 = N_i(t), \tag{4.3.2}$$

we obtain that, properly normalized, it is given as

$$\Phi_i(\vec{x},t) = \sqrt{N_i(t)} \prod_{j=1,2} \left(\frac{1}{\pi q_{i,x_j}^2(t)}\right)^{\frac{1}{4}} \exp\left(-\frac{x_j^2}{2q_{i,x_j}^2(t)}\left(1 - i\frac{m_{x_j} q_{i,x_j}(t)}{\hbar}\frac{\mathrm{d}q_{i,x_j}}{\mathrm{d}t}\right) + \frac{i}{2}\theta_i(t)\right). \tag{4.3.3}$$

Let us consider the continuity equation

$$\frac{\partial}{\partial t}|\Phi_i(\vec{x},t)|^2 + \vec{\nabla}\cdot\vec{j_i} = 0, \tag{4.3.4}$$

with

$$j_{i,x_j} = |\Phi_i(\vec{x},t)|^2 \vec{v_s}(\vec{x},t) = \frac{\hbar}{2m_{x_j} i}\left(\Phi_i^*(\vec{x},t)\partial_{x_j}\Phi_i(\vec{x},t) - \Phi_i(\vec{x},t)\partial_{x_j}\Phi_i^*(\vec{x},t)\right), \tag{4.3.5}$$

where $\vec{v_s}(\vec{x},t)$ is the superfluid velocity. To check the Gaussian ansatz we will check if eqn. (4.3.4) is obeyed if we set the pumping parameter ν to zero. If there is no pumping the number of particles in both valleys does not change, i.e. $\frac{\mathrm{d}N_i}{\mathrm{d}t}=0$. Writing out the continuity equation yields

$$\begin{aligned}\frac{\partial}{\partial t}|\Phi_i(\vec{x},t)|^2 &= \frac{\partial}{\partial t}\left[N_i(t)\prod_{j=1,2}\left(\frac{1}{\pi q_{i,x_j}^2(t)}\right)^{\frac{1}{2}}\exp\left(-\frac{x_j^2}{q_{i,x_j}^2(t)}\right)\right]\\ &= N_i(t)\sum_{l=1,2}\left[\left(\frac{1}{q_{i,x_l}(t)}\frac{\mathrm{d}q_{i,x_l}}{\mathrm{d}t}\right)\left(1-\frac{2x_l^2}{q_{i,x_l}^2(t)}\right)\right]\prod_{j=1,2}\left(\frac{1}{\pi q_{i,x_j}^2(t)}\right)^{\frac{1}{2}}\exp\left(-\frac{x_j^2}{q_{i,x_j}^2(t)}\right),\end{aligned} \tag{4.3.6}$$

and

$$\begin{aligned}\vec{\nabla}\cdot\vec{j_i} &= \sum_{l=1,2}\left[N_i(t)\partial_{x_l}\left(\left(\frac{x_l}{q_{i,x_l}(t)}\frac{\mathrm{d}q_{i,x_l}}{\mathrm{d}t}\right)\prod_{j=1,2}\left(\frac{1}{\pi q_{i,x_j}^2(t)}\right)^{\frac{1}{2}}\exp\left(-\frac{x_j^2}{q_{i,x_j}^2(t)}\right)\right)\right]\\ &= N_i(t)\sum_{l=1,2}\left[\left(\frac{1}{q_{i,x_l}(t)}\frac{\mathrm{d}q_{i,x_l}}{\mathrm{d}t}\right)\left(1-\frac{2x_l^2}{q_{i,x_l}^2(t)}\right)\right]\prod_{j=1,2}\left(\frac{1}{\pi q_{i,x_j}^2(t)}\right)^{\frac{1}{2}}\exp\left(-\frac{x_j^2}{q_{i,x_j}^2(t)}\right),\end{aligned} \tag{4.3.7}$$

thus it is indeed obeyed.

4.4 Steady-state stability analysis

To take the finite width and length of the film of YIG into account we add two single particle harmonic oscillators (one for each spatial dimension) to the energy functional in eqn. (4.1.9) and obtain

$$\begin{aligned}\epsilon[\Phi,\Phi^*] = \int \mathrm{d}\vec{x}\Big[&\Phi_1^*\hbar\omega(\partial_{\vec{x}})\Phi_1+\Phi_2^*\hbar\omega(\partial_{\vec{x}})\Phi_2-\mu\left(\Phi_1^*\Phi_1+\Phi_2^*\Phi_2\right)+\boldsymbol{\nu}^*\Phi_1^*\Phi_2^*\\ &+\boldsymbol{\nu}\Phi_1\Phi_2+\frac{\gamma_1}{2}\left(\Phi_1^*\Phi_1+\Phi_2^*\Phi_2\right)^2+\frac{\gamma_2}{2}\left(\Phi_1^*\Phi_1-\Phi_2^*\Phi_2\right)^2\\ &+\frac{1}{2}\left(m_{x_1}\omega_{x_1}^2x_1^2+m_{x_2}\omega_{x_2}^2x_2^2\right)\left(\Phi_1^*\Phi_1+\Phi_2^*\Phi_2\right)\Big],\end{aligned} \tag{4.4.1}$$

with $\omega_{x_j}=\omega_{\mathbf{k}_{0,j}}-\omega_{\mathbf{k}_0}$, where $\mathbf{k}_{0,j}=\mathbf{k}_0+\frac{\pi}{L_{x_j}}\hat{x_j}$ and L_{x_j} is the width of the film of YIG in the x_j-direction.

By plugging the Gaussian ansatz into the energy functional in eqn. (4.4.1) and assuming the steady-state situation, i.e. $\frac{\mathrm{d}q_{i,x_j}}{\mathrm{d}t}=0$, we obtain

$$
\begin{aligned}
\epsilon\left[N_1,\, N_2, \vec{q_1}, \vec{q_2}, \theta_1, \theta_2\,\right] = \\
&\sum_{i=1,2}\left[\left(\hbar\omega_{\vec{k}_0} + \sum_{j=1,2}\frac{\hbar^2}{4m_{x_j}q_{i,x_j}^2}\right)N_i\right] \\
&- \mu\left(N_1+N_2\right) + \nu\sqrt{N_1N_2}\cos\left(\theta_1+\theta_2+\theta_\nu\right)\prod_{j=1,2}\frac{\sqrt{q_{1,x_j}q_{2,x_j}}}{\sqrt{q_{1,x_j}^2+q_{2,x_j}^2}} \\
&+ \frac{\gamma_1}{4\pi}\left(\frac{N_1^2}{q_{1,x_1}q_{1,x_2}} + \frac{2N_1N_2}{\sqrt{(q_{1,x_1}^2+q_{2,x_1}^2)(q_{1,x_2}^2+q_{2,x_2}^2)}} + \frac{N_2^2}{q_{2,x_1}q_{2,x_2}}\right) \\
&+ \frac{\gamma_2}{4\pi}\left(\frac{N_1^2}{q_{1,x_1}q_{1,x_2}} - \frac{2N_1N_2}{\sqrt{(q_{1,x_1}^2+q_{2,x_1}^2)(q_{1,x_2}^2+q_{2,x_2}^2)}} + \frac{N_2^2}{q_{2,x_1}q_{2,x_2}}\right) \\
&+ \frac{1}{2}\sum_{i,j=1,2}\left[\frac{m_{x_j}\omega_{x_j}^2q_{i,x_j}^2}{2}N_i\right],
\end{aligned}
\tag{4.4.2}
$$

where we have rewritten $\boldsymbol{\nu} = \nu e^{i\theta_\nu}$.

We can read-off from this expression that minimizing with respect to θ_i will yield that $\theta_1 + \theta_2 = -\theta_\nu + k\pi$, with $k \in \{1, 3\}$. To further simplify we approximate our system by assuming that the dispersion is isotropic and that the lattice width in the x_1 and x_2-direction are equal. From this it follows that $m_{x_1} = m_{x_2} \equiv m$ and $\omega_{x_1} = \omega_{x_2} \equiv \omega$. If we consider a system for which it holds that $q_{i,x_1} = q_{i,x_2}$ we obtain that the steady-state energy functional in eqn. (4.4.2) will transform to the isotropic, steady-state energy functional as

$$
\begin{aligned}
\epsilon\left[N_1, N_2, q_1, q_2\right] = \sum_{i=1,2}\left[\left(\hbar\omega_{\vec{k}_0} - \mu + \frac{\hbar^2}{2mq_i^2} + \frac{m\omega^2q_i^2}{2}\right)N_i\right] \\
- \nu\frac{\sqrt{N_1N_2}q_1q_2}{q_1^2+q_2^2} + \frac{\gamma_1+\gamma_2}{4\pi}\left(\frac{N_1^2}{q_1^2} + \frac{N_2^2}{q_2^2}\right) + \frac{\gamma_1-\gamma_2}{2\pi}\frac{N_1N_2}{q_1^2+q_2^2}.
\end{aligned}
\tag{4.4.3}
$$

4.4.1 Single BEC

If there is no pumping and only one valley is occupied we obtain that the energy functional in eqn. (4.4.3) is given as

$$
\epsilon\left[N, q\right] = \left(\hbar\omega_{\vec{k}_0} - \mu + \frac{\hbar^2}{2mq^2} + \frac{m\omega^2q^2}{2}\right)N + \frac{\gamma_1+\gamma_2}{4\pi}\frac{N^2}{q^2},
\tag{4.4.4}
$$

with $N = N_1$ and $q = q_1$. In the isotropic, steady-state case with only one valley occupied and without pumping the dimensionless energy functional is

$$\epsilon\left[q\right] = \frac{1}{2q^2} + \frac{q^2}{2} + \frac{\Gamma_{\text{in}} N}{2q^2}, \tag{4.4.5}$$

with $\Gamma_{\text{in}} = \frac{(\gamma_1+\gamma_2)m}{2\pi\hbar^2}$. We rescaled the Gaussian widths by the harmonic oscillator length, $l = \sqrt{\frac{\hbar}{m\omega}}$ and divided the energy by $N\hbar\omega$. Note that we dropped terms in the energy functional that do not depend on q, since we are only interested in energy differences. Performing a stability analysis of ϵ w.r.t. q yields

$$\frac{\partial \epsilon}{\partial q} = \frac{-1}{q^3} + q - \frac{\Gamma_{\text{in}} N}{q^3} = 0. \tag{4.4.6}$$

We find that

$$q = \left(1 + \Gamma_{\text{in}} N\right)^{\frac{1}{4}} \tag{4.4.7}$$

Now we perform the second partial derivative test and apply the condition on the stationary point for it to be a stable minimum, i.e.

$$\frac{\partial^2 \epsilon}{\partial q^2} = \frac{3}{q^4} + 1 + \frac{3\Gamma_{\text{in}} N}{q^4} > 0. \tag{4.4.8}$$

Evaluating this condition in the value for q as given in eqn. (4.4.7) yields the condition that

$$\Gamma_{\text{in}} N > -1. \tag{4.4.9}$$

In Fig. 4.1 the the energy as a function of the Gaussian width is depicted for three different values of $\Gamma_{\text{in}} N$. This figure clearly shows that if the condition in eqn. (4.4.9) is satisfied there is a stable solution for the static system and if the condition is not satisfied the system will be unstable and probably collapse.

4.4.2 Two symmetric condensates

In the isotropic, steady-state case where both valleys are equally occupied and there is no pumping the dimensionless energy functional derived from eqn. (4.4.3) is

$$\epsilon\left[q_1, q_2\right] = \frac{1}{2q_1^2} + \frac{1}{2q_2^2} + \frac{q_1^2 + q_2^2}{2} + \Gamma_1 \left(\frac{1}{2q_1^2} + \frac{1}{q_1^2 + q_2^2} + \frac{1}{2q_2^2}\right) + \Gamma_2 \left(\frac{1}{2q_1^2} - \frac{1}{q_1^2 + q_2^2} + \frac{1}{2q_2^2}\right), \tag{4.4.10}$$

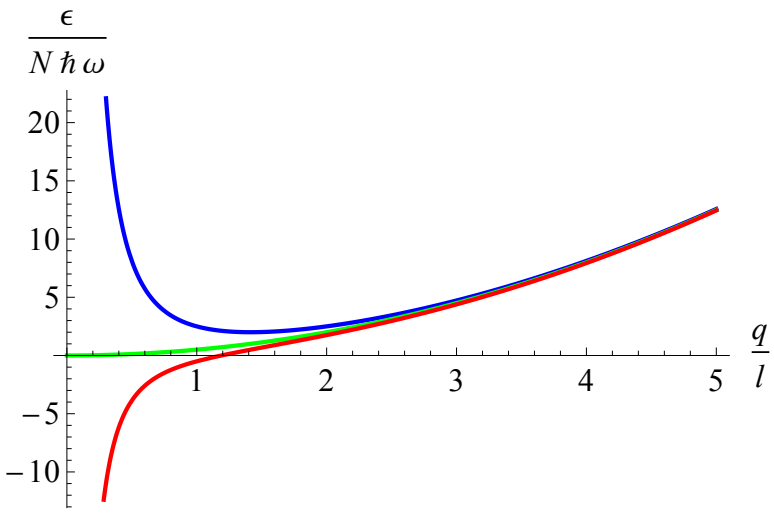

Figure 4.1: The energy as function of the Gaussian width for three different values of $\Gamma_{\text{in}}N$. The blue line corresponds to $\Gamma_{\text{in}}N = 3$, the green line to $\Gamma_{\text{in}}N = -1$ and the red line to $\Gamma_{\text{in}}N = -3$.

with $\Gamma_i = \frac{\gamma_i m N}{2\pi\hbar^2}$. Doing stability analysis w.r.t. q_1 and q_2, thus first solving stationary points yields

$$\frac{\partial \epsilon}{\partial q_1} = -\frac{1}{q_1^3} + q_1 + \Gamma_1\left(-\frac{1}{q_1^3} - \frac{2q_1}{\left(q_1^2+q_2^2\right)^2}\right) + \Gamma_2\left(-\frac{1}{q_1^3} + \frac{2q_1}{\left(q_1^2+q_2^2\right)^2}\right) = 0, \tag{4.4.11}$$

$$\frac{\partial \epsilon}{\partial q_2} = -\frac{1}{q_2^3} + q_2 + \Gamma_1\left(-\frac{2q_2}{\left(q_1^2+q_2^2\right)^2} - \frac{1}{q_2^3}\right) + \Gamma_2\left(\frac{2q_2}{\left(q_1^2+q_2^2\right)^2} - \frac{1}{q_2^3}\right) = 0. \tag{4.4.12}$$

Solving for q_1 and q_2 yields

$$q_1 = \left(1 + \frac{3}{2}\Gamma_1 + \frac{1}{2}\Gamma_2\right)^{\frac{1}{4}}, \tag{4.4.13}$$

$$q_2 = \left(1 + \frac{3}{2}\Gamma_1 + \frac{1}{2}\Gamma_2\right)^{\frac{1}{4}}, \tag{4.4.14}$$

hence we only find a stationary point if $3\Gamma_1 + \Gamma_2 > -2$. Now perform the second partial derivative test and obtain the conditions for the stationary

point to be a stable minimum as

$$\frac{\partial^2 \epsilon}{\partial q_1^2} = \frac{8 + 10\Gamma_1 + 6\Gamma_2}{2 + 3\Gamma_1 + \Gamma_2} > 0, \tag{4.4.15a}$$

$$\frac{\partial^2 \epsilon}{\partial q_1^2}\frac{\partial^2 \epsilon}{\partial q_2^2} - \left(\frac{\partial^2 \epsilon}{\partial q_1 \partial q_2}\right)^2 = \frac{32\,(1 + \Gamma_1 + \Gamma_2)}{2 + 3\Gamma_1 + \Gamma_2} > 0. \tag{4.4.15b}$$

Combining the condition that there is a stationary point and the condition in eqn. (4.4.15b) yields that there is a stable minimum if $\Gamma_1 > -\frac{1}{2}$ and $\Gamma_2 > -\Gamma_1 - 1$ or if $\Gamma_1 < -\frac{1}{2}$ and $\Gamma_2 > -3\Gamma_1 - 2$. The condition in eqn. (4.4.15a) is automatically obeyed if the other two conditions are obeyed. In Fig. 4.2 a stable solution and an unstable solution are depicted.

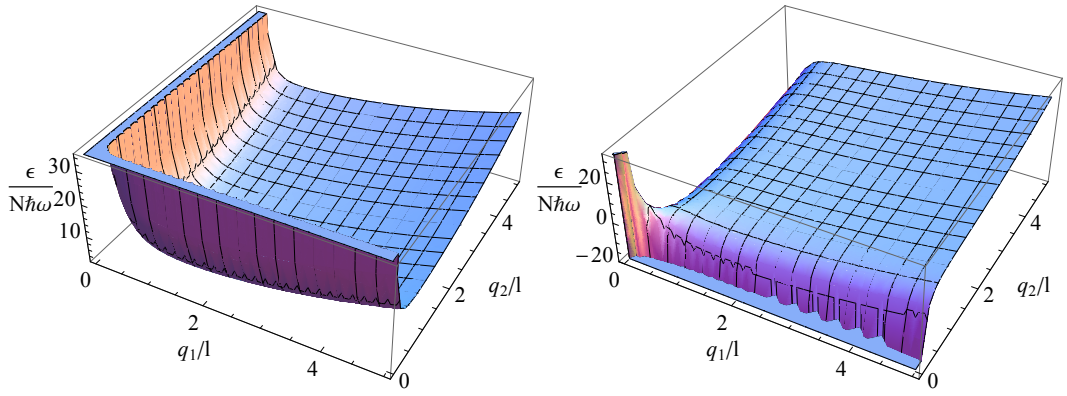

(a) $\Gamma_1 = 1$ and $\Gamma_2 = -1$, stable. (b) $\Gamma_1 = 1$ and $\Gamma_2 = -4$, unstable.

Figure 4.2: The energy as function of the Gaussian widths for a stable and an unstable system.

In the case where both valleys are equally occupied and pumping is taken into account, the dimensionless energy, with ν divided by $\hbar\omega$, derived from eqn. (4.4.3) is given by

$$\begin{aligned}\epsilon\,[N, q_1, q_2] = &\frac{1}{2q_1^2} + \frac{1}{2q_2^2} + \frac{q_1^2 + q_2^2}{2} - \nu\frac{q_1 q_2}{q_1^2 + q_2^2} \\ &+ \Gamma_1\left(\frac{1}{2q_1^2} + \frac{1}{q_1^2 + q_2^2} + \frac{1}{2q_2^2}\right) + \Gamma_2\left(\frac{1}{2q_1^2} - \frac{1}{q_1^2 + q_2^2} + \frac{1}{2q_2^2}\right).\end{aligned} \tag{4.4.16}$$

Note that the term corresponding to pumping is $\nu\frac{q_1 q_2}{q_1^2+q_2^2}$. Recall that without pumping there was at most one minimum for which $q_1 = q_2$. Note that the pumping term minimizes the energy when $q_1 = q_2$, thus minima obey $q_1 = q_2$. However if $q_1 = q_2$ the pumping term only gives a constant contribution to the energy thus the position of the minimum does not move due to the pumping, hence the solutions are the same as in Subsection 4.4.2.

4.5 Equations of motion

In order to study the dynamics we will deduce equations of motion (EoM) for Φ and we will show two different ways to do so. The first method begins with considering the Landau-Lifshitz-Gilbert (LLG) equation

$$\frac{\partial\vec{\Omega}(\vec{x},t)}{\partial t} = \vec{\Omega}(\vec{x},t) \times \left(-\frac{1}{\hbar}\frac{\delta\epsilon\left[\Omega\right]}{\delta\vec{\Omega}(\vec{x},t)} \right) - \alpha\vec{\Omega}(\vec{x},t) \times \frac{\partial\vec{\Omega}(\vec{x},t)}{\partial t}, \tag{4.5.1}$$

with $\vec{\Omega}(\vec{x},t) = \frac{1}{S}\vec{S}(\vec{x,t})$ the normalized spin vector and $\alpha > 0$ the Gilbert damping. The LLG equation is an equation of motion for the magnetization. If $\alpha = 0$, then the magnetic energy is a constant of motion for the LLG equation. However we expect that the equilibrium situation is such that the magnetization points along the effective magnetic field and the magnetic energy is minimized. Therefore the term proportional to α, i.e. the Gilbert damping term, is constructed such that the direction of magnetization spirals towards the effective magnetic field while precessing. Note that the length of the vector $\vec{\Omega}$ is also a constant of motion of the LLG equation [16].

By plugging the Holstein-Primakoff transformation up to fourth order for $\vec{S}(\vec{x},t)$ into the LLG equation we obtain the equation of motion for $\Phi_i(\vec{x},t)$

$$i\hbar\left(1 + i\alpha\right)\frac{\partial\Phi_i}{\partial t} = \frac{\delta\epsilon}{\delta\Phi_i^*}. \tag{4.5.2}$$

An alternative way is by using an adjusted variational principle. The action of our system is

$$\mathcal{S} = \int \mathrm{d}t \left(\int \mathrm{d}\vec{x}\left(\Phi_1^* i\hbar\partial_t\Phi_1 + \Phi_2^* i\hbar\partial_t\Phi_2\right) - \epsilon\left[\Phi,\Phi^*\right] \right). \tag{4.5.3}$$

We introduce the Rayleigh dissipation function

$$\mathcal{R} = \alpha \int \mathrm{d}t \int \mathrm{d}\vec{x}\left(|\partial_t\Phi_1|^2 + |\partial_t\Phi_2|^2\right), \tag{4.5.4}$$

with α the Gilbert damping term, which plays a role similar to the Gilbert damping term in the LLG equation. Without the Gilbert damping term the magnetic energy would be a constant of motion, which would prevent the system for moving towards its expected equilibrium situation. From the action and the Rayleigh dissipation function we can also obtain the equation of motion for $\Phi_i(\vec{x},t)$, but this time from the variational principle, i.e.

$$\frac{\delta\mathcal{S}}{\delta\Phi_i^*} = \frac{\delta\mathcal{R}}{\delta\left(\partial_t\Phi_i^*\right)}, \tag{4.5.5}$$

and we indeed obtain eqn. (4.5.2). By performing the functional derivatives in eqn. (4.5.2) we obtain

$$\begin{aligned} i\hbar\,(1+i\alpha)\frac{\partial}{\partial t}|\Phi\rangle = \\ &\left(\hbar\omega_{\mathbf{k}_0} - \mu - \frac{\hbar^2\partial_{x_1}^2}{2m_{x_1}} - \frac{\hbar^2\partial_{x_2}^2}{2m_{x_2}} + \frac{1}{2}m_{x_1}\omega_{x_1}^2 x_1^2 + \frac{1}{2}m_{x_2}\omega_{x_2}^2 x_2^2\right)|\Phi\rangle \\ &+ \boldsymbol{\nu}^*\sigma_x|\Phi^\dagger\rangle + \gamma_1\langle\Phi|\Phi\rangle|\Phi\rangle + \gamma_2\langle\Phi|\sigma_z|\Phi\rangle\sigma_z|\Phi\rangle, \end{aligned} \tag{4.5.6}$$

with $|\Phi\rangle = \begin{pmatrix}\Phi_1\\ \Phi_2\end{pmatrix}$, $\langle\Phi| = (\Phi_1^*, \Phi_2^*)$, and σ_i the Pauli spin matrices.

4.6 EoM in Gaussian ansatz for single BEC

We will use the equations of motion for Φ as derived in the previous section to obtain equations of motion for the parameters from the Gaussian anzatz earlier introduced. We consider a system which is isotropic, where only one valley is occupied and without pumping. The Gaussian ansatz then is

$$\Phi(\vec{x},t) = \sqrt{N(t)}\frac{1}{\sqrt{\pi}q(t)}\exp\left(-\frac{x_1^2+x_2^2}{2q^2(t)}\left(1-\frac{im}{\hbar}q(t)\dot{q}(t)\right)+i\theta(t)\right). \tag{4.6.1}$$

By plugging this ansatz into eqn. (4.4.1) we obtain that the energy functional for this system is

$$\epsilon\,[N,q,\dot{q}] = \left(\hbar\omega_{\vec{k}_0} - \mu + \frac{\hbar^2}{2mq^2} + \frac{m}{2}\dot{q}^2 + \frac{m\omega^2q^2}{2}\right)N + \frac{\gamma_1+\gamma_2}{4\pi}\frac{N^2}{q^2} = T\,[N,\dot{q}] + V\,[N,q]\,, \tag{4.6.2}$$

where we left out the explicit time-dependence for notational convenience. To obtain equations of motion there are several methods available.

4.6.1 Normalization

The first method is by applying ∂_t on the normalization equation for Φ as

$$\dot{N}(t) = \partial_t\int \mathrm{d}^2x|\Phi(\vec{x},t)|^2, \tag{4.6.3}$$

then inserting the equations of motion for Φ and Φ^* obtained from eqn. (4.5.6), and performing the spatial integrals in order to obtain

$$\begin{aligned}\dot{N} &= -\frac{2\alpha\,(\hbar\omega_{\mathbf{k}_0}-\mu)\,N}{(1+\alpha^2)\,\hbar} - \frac{\alpha\hbar N}{m\,(1+\alpha^2)\,q^2} - \frac{\alpha\,(\gamma_1+\gamma_2)\,N^2}{(1+\alpha^2)\,\hbar\pi q^2} - \frac{\alpha m\omega^2 N q^2}{(1+\alpha^2)\,\hbar} - \frac{\alpha m N\dot{q}^2}{(1+\alpha^2)\,\hbar} \\ &= -\frac{2\alpha N}{(1+\alpha^2)\,\hbar}\frac{\partial\epsilon}{\partial N}. \end{aligned} \tag{4.6.4}$$

4.6.2 Projection of the EoM

The second method is the projection method. From the equations of motion for Φ we obtain by "projection" that

$$\begin{aligned}
\int \mathrm{d}\vec{x} \frac{\partial \Phi^*}{\partial N} i\hbar \left(1 + i\alpha\right) \partial_t \Phi &= \int \mathrm{d}\vec{x} \frac{\partial \Phi^*}{\partial N} \frac{\delta \epsilon}{\delta \Phi^*}, \\
\int \mathrm{d}\vec{x} \frac{\partial \Phi^*}{\partial \theta} i\hbar \left(1 + i\alpha\right) \partial_t \Phi &= \int \mathrm{d}\vec{x} \frac{\partial \Phi^*}{\partial \theta} \frac{\delta \epsilon}{\delta \Phi^*}, \\
\int \mathrm{d}\vec{x} \frac{\partial \Phi^*}{\partial q} i\hbar \left(1 + i\alpha\right) \partial_t \Phi &= \int \mathrm{d}\vec{x} \frac{\partial \Phi^*}{\partial q} \frac{\delta \epsilon}{\delta \Phi^*}.
\end{aligned} \tag{4.6.5}$$

We use the Gaussian ansatz, perform the spatial integrals, split real and imaginary parts and simplify in order to obtain equations of motion for $N(t)$, $q(t)$ and $\theta(t)$ as

$$\dot{N} = -\frac{2\alpha N}{(1+\alpha^2)\hbar} \frac{\partial \epsilon}{\partial N}, \tag{4.6.6a}$$

$$\dot{\theta} = -\frac{1}{2\hbar} m q \ddot{q} + \frac{1}{2\hbar} m \dot{q}^2 - \frac{1}{(1+\alpha^2)\hbar} \frac{\partial \epsilon}{\partial N}, \tag{4.6.6b}$$

$$mN\ddot{q} = -\frac{\partial \epsilon}{\partial q} - 2\alpha\hbar N \frac{\dot{q}}{q^2} - \frac{\alpha m^2}{2\hbar} N \dot{q}^3 + \frac{\alpha m^2}{2\hbar} N q \dot{q} \ddot{q}, \tag{4.6.6c}$$

$$mN\ddot{q} = -\frac{\partial \epsilon}{\partial q} - \frac{2\alpha\hbar N}{q\dot{q}} \ddot{q}. \tag{4.6.6d}$$

Note that we obtain two equations of motion for q. We will drop the terms containing third order time-derivatives in eqn. (4.6.6c), because the LLG equation as given in eqn. (4.5.1) only contains a damping term that has a first order time-derivative. The next order damping term we could add to the LLG equation would be third order in time derivatives, because it has to break time-reversal symmetry since it is a damping term. Since our original equation of motion does not take third and higher order time derivatives into account, it would not be reasonable to do so here. The remaining damping terms in the two equations of motion for q are equal if q would be an oscillating function. The damping term in eqn. (4.6.6c) agrees with previous results [17] and it can be interpreted as a friction term in this form, thus it

is reasonable to assume that the correct equations of motion are

$$\dot{N} = -\frac{2\alpha N}{(1+\alpha^2)\hbar}\frac{\partial \epsilon}{\partial N}, \tag{4.6.7a}$$

$$\dot{\theta} = -\frac{1}{2\hbar}mq\ddot{q} + \frac{1}{2\hbar}m\dot{q}^2 - \frac{1}{(1+\alpha^2)\hbar}\frac{\partial \epsilon}{\partial N}, \tag{4.6.7b}$$

$$mN\ddot{q} = -\frac{\partial \epsilon}{\partial q} - 2\alpha\hbar N\frac{\dot{q}}{q^2}. \tag{4.6.7c}$$

4.6.3 Variational principle

The last method we consider is based on using the variational principle combined with the use of the Rayleigh dissipation functional. For the isotropic system, without pumping and when only one valley is occupied we obtain by using the Gaussian ansatz from eqn. (4.6.1) that the action is

$$\mathcal{S} = \int \mathrm{d}t \left[\left(\frac{i\hbar}{2}\dot{N} - \hbar N\dot{\theta} + \frac{m}{2}N\dot{q}^2 - \frac{m}{2}Nq\ddot{q} - \epsilon\left[N, q, \dot{q}\right] \right], \tag{4.6.8}$$

and the Rayleigh dissipation functional is

$$\mathcal{R} = \alpha\hbar \int \mathrm{d}t \left[\frac{\dot{N}^2}{4N} + N\dot{\theta}^2 + N\frac{\dot{q}^2}{q^2} + \frac{mN}{\hbar}\left(q\dot{\theta}\ddot{q} - \dot{\theta}\dot{q}^2 + \frac{m}{2\hbar}\dot{q}^4 + \frac{m}{2\hbar}q^2\ddot{q}^2 - \frac{m}{\hbar}q\dot{q}^2\ddot{q} \right) \right]. \tag{4.6.9}$$

We again drop third and higher order time derivative terms using the same argument as we used with the projection method

$$\mathcal{R} = \alpha\hbar \int \mathrm{d}t \left[\frac{\dot{N}^2}{4N} + N\dot{\theta}^2 + N\frac{\dot{q}^2}{q^2} \right]. \tag{4.6.10}$$

We should obtain the equations of motion from

$$\begin{aligned} \frac{\delta \mathcal{S}}{\delta N} &= \frac{\delta \mathcal{R}}{\delta \dot{N}}, \\ \frac{\delta \mathcal{S}}{\delta \theta} &= \frac{\delta \mathcal{R}}{\delta \dot{\theta}}, \\ \frac{\delta \mathcal{S}}{\delta q} &= \frac{\delta \mathcal{R}}{\delta \dot{q}}. \end{aligned} \tag{4.6.11}$$

However, for not yet understood reasons, the extension of the variational principle from eqn. (4.5.5) does not give results corresponding to those obtained by the two previously discussed methods.

4.6.4 Damping and interaction

Making the equations of motion in eqn. (4.6.7) dimensionless yields

$$\dot{N} = -\frac{2\alpha N}{1+\alpha^2}\left(\frac{\hbar\omega_{\mathbf{k}_0}-\mu}{\hbar\omega} + \frac{1}{2q^2} + \frac{1}{2}\dot{q}^2 + \frac{1}{2}q^2 + \frac{\Gamma_{\text{in}}N}{q^2}\right), \tag{4.6.12a}$$

$$\dot{\theta} = -\frac{1}{2}q\ddot{q} + \frac{1}{2}\dot{q}^2 - \frac{1}{1+\alpha^2}\left(\frac{\hbar\omega_{\mathbf{k}_0}-\mu}{\hbar\omega} + \frac{1}{2q^2} + \frac{1}{2}\dot{q}^2 + \frac{1}{2}q^2 + \frac{\Gamma_{\text{in}}N}{q^2}\right), \tag{4.6.12b}$$

$$\ddot{q} = \frac{1}{q^3} - q + \frac{\Gamma_{\text{in}}N}{q^3} - 2\alpha\frac{\dot{q}}{q^2}. \tag{4.6.12c}$$

Recall from Subsection 4.4.1 that $\Gamma_{\text{in}} = \frac{m(\gamma_1+\gamma_2)}{2\pi\hbar^2}$.

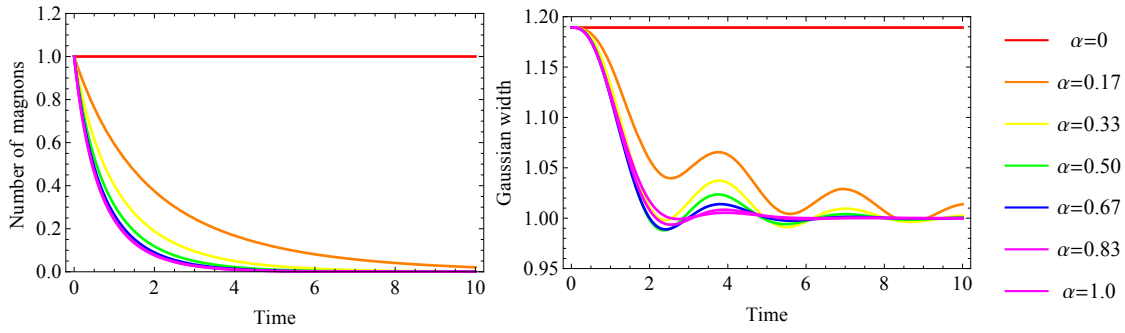

(a) (b)

Figure 4.3: In (a) and (b) are respectively plotted the number of magnons, N, and the Gaussian width, $\frac{q}{l}$, against the time, ωt, for different values of the Gilbert damping and with $\Gamma_{\text{in}} = -\frac{1}{2}$.

In Fig. 4.3 plots of the numerical solutions for the equations of motion in eqn. (4.6.12) are depicted for different values of α, with $\Gamma_{\text{in}} = -\frac{1}{2}$. We set $\hbar\omega_{\mathbf{k}_0} - \mu = 0$, because we assume the system to be in a BEC. We chose $q(0) = (1+\Gamma_{\text{in}})^{\frac{1}{4}}$ and $\dot{q}(0) = 0$ as in correspondence with the stability analysis done in Subsection 4.4.1. In Fig. 4.3a and Fig. 4.3b respectively the number of magnons, N, and the Gaussian width, q, are plotted against the time. To determine whether or not the depicted solutions are stable, i.e. if the density does not diverge, we focus on $\frac{N}{q^2}$, because it provides a good measure for the density of magnons in the valley. From the figures it can be read off that the density converges. For $\alpha = 0$ the system does not change in time. For the other values of α the number of magnons decreases to zero and the Gaussian width behaves like a damped oscillator that goes to $q = 1$, thus the density goes to zero. Hence all of these solutions are stable.

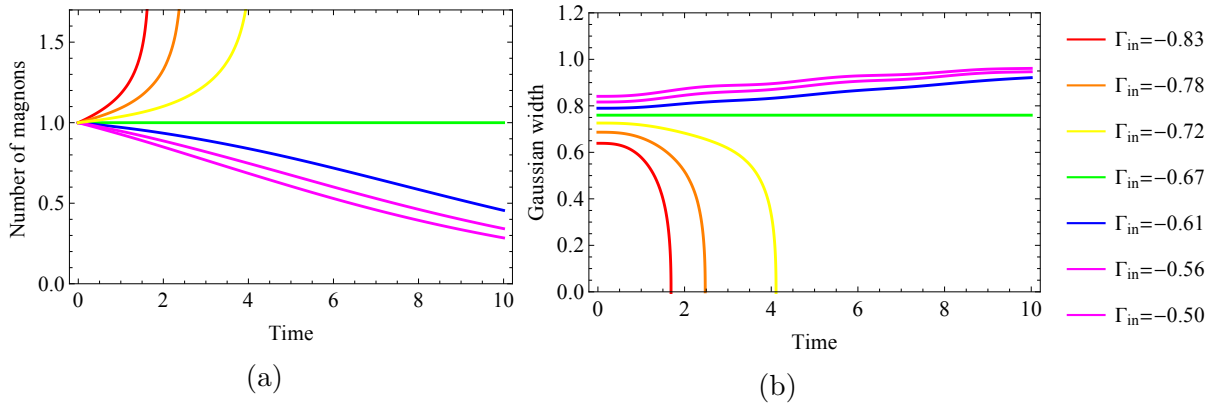

(a) (b)

Figure 4.4: In (a) and (b) are respectively plotted the number of magnons, N, and the Gaussian width, $\frac{q}{l}$, against the time, ωt, for different values of the interaction and with $\alpha = 0.1$

In Fig. 4.4 numerical solutions are shown with varying interaction, Γ_{in}, and fixed damping, $\alpha = 0.1$. For $\Gamma_{\text{in}} = -\frac{2}{3}$ the system does not change in time. For $\Gamma_{\text{in}} > -\frac{2}{3}$ the number of magnons decreases and the Gaussian width goes to $q = 1$, hence the density goes to zero, thus the system is stable. For $\Gamma_{\text{in}} < -\frac{2}{3}$ the number of magnons increases and the Gaussian width decreases to 0. Hence the density, $\frac{N}{q^2}$, diverges, which indicates a collapse of the BEC. From the equations of motion in eqn. (4.6.12) we find that whether or not the system is stable does not depend on the damping but depends on the interaction.

4.6.5 A pumped BEC

Consider the equations of motion in eqn. (4.6.12), add pumping to the system and assume that the pumping only changes the equation of motion for N as

$$\dot{N} = -\frac{2\alpha N}{1+\alpha^2}\left(\frac{\hbar\omega_{\mathbf{k}_0} - \mu}{\hbar\omega} + \frac{1}{2q^2} + \frac{1}{2}\dot{q}^2 + \frac{1}{2}q^2 + \frac{\Gamma_{\text{in}} N}{q^2}\right) + \nu, \qquad (4.6.13)$$

with ν the pumping parameter dimensionless.

In Fig. 4.5 plots of the number of magnons and the Gaussian width are depicted with fixed interaction, $\Gamma_{\text{in}} = -\frac{1}{2}$, and damping, $\alpha = 0.1$, and varying pumping. We can read off that for higher pumping frequencies the system becomes unstable but for lower pumping the system is not. Due to the pumping the number of magnons will not go to zero but decreases to a stable value.

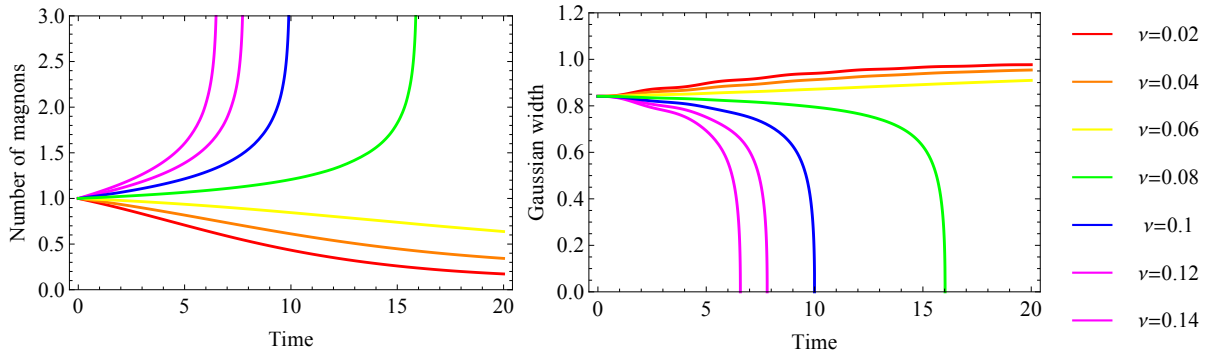

(a) (b)

Figure 4.5: In (a) and (b) are respectively plotted the number of magnons, N, and the Gaussian width, $\frac{q}{l}$, against the time, ωt, for different values of the pumping and with $\alpha = 0.1$ and $\Gamma_{\text{in}} = -\frac{1}{2}$.

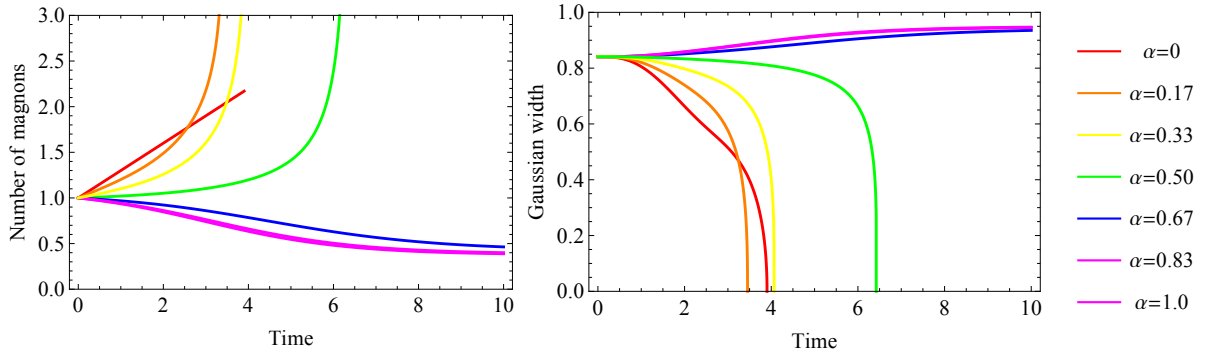

(a) (b)

Figure 4.6: In (a) and (b) are respectively plotted the number of magnons, N, and the Gaussian width, $\frac{q}{l}$, against the time, ωt, for different values of the damping and with $\Gamma_{\text{in}} = -\frac{1}{2}$ and $\nu = 0.3$.

In Fig. 4.6 the same values for α and Γ_{in} have been used as in Fig. 4.3 but now we have added pumping, with $\nu = 0.3$. We can read off that the pumping causes the systems with lower damping to become unstable, while the systems with higher damping remain stable.

The final result for the analysis of the stability of the one valley system with pumping is given in Fig. 4.7. Shown is whether or not the system is stable depending on the damping and the pumping for different values of the interaction. One can read off that as the interaction becomes more attractive, i.e. Γ_{in} becomes more negative, the region where the system is stable decreases in area. If the interaction is strong enough then even for high

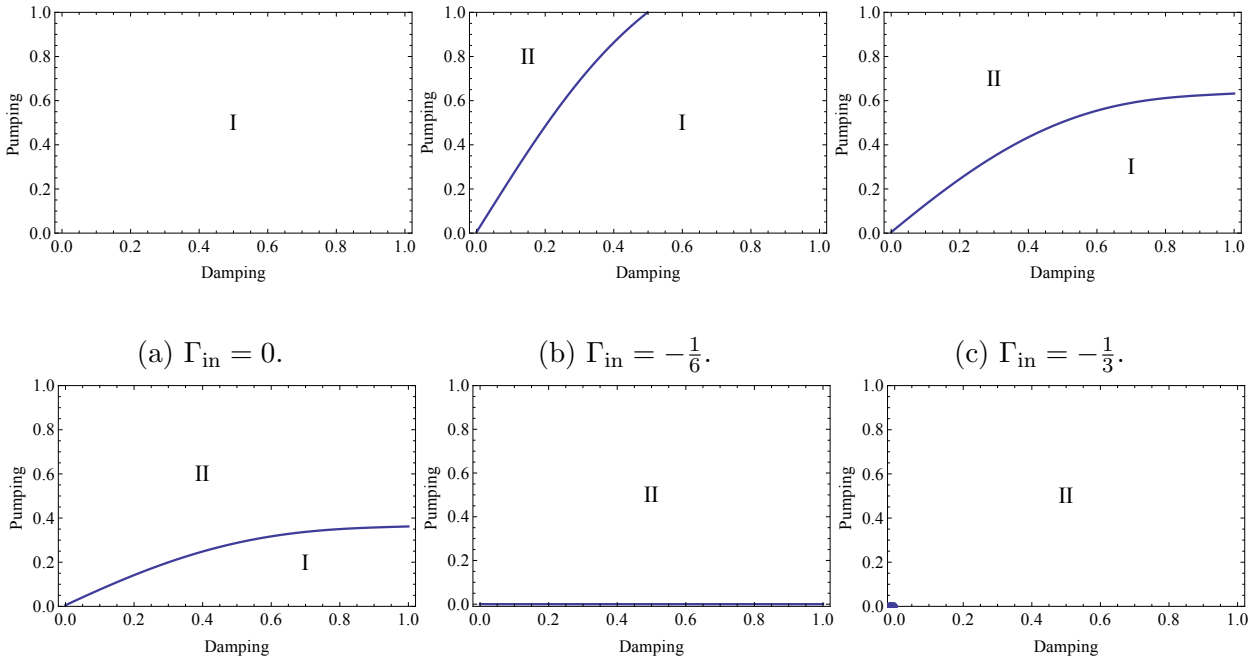

(a) $\Gamma_{\text{in}} = 0$. (b) $\Gamma_{\text{in}} = -\frac{1}{6}$. (c) $\Gamma_{\text{in}} = -\frac{1}{3}$.

(d) $\Gamma_{\text{in}} = -\frac{1}{2}$. (e) $\Gamma_{\text{in}} = -\frac{2}{3}$. (f) $\Gamma_{\text{in}} = -\frac{5}{6}$.

Figure 4.7: Plotted are the regions of values for the damping and the pumping for which the system is stable, I, and for which the system is unstable, II.

damping and low pumping the system becomes unstable. We can also read off that the boundary between the stable and unstable regions is a monotonically increasing line with a monotonically decreasing inclination. Hence higher damping does make the system "more" stable, but the influence on the system of increased damping decreases for higher values of the damping.

4.7 Two pumped BEC's

Let us consider the isotropic system, but now with both valleys occupied and also include pumping. By plugging the Gaussian ansatz of eqn. (4.3.3) into

the energy functional of eqn. (4.4.1) and setting $q_{i,x_1} = q_{i,x_2}$ we obtain that

$$\epsilon\left[N_1, N_2, q_1, q_2, \theta_1, \theta_2\right] = \sum_{i=1,2}\left[\left(\hbar\omega_{\vec{k}_0} + \frac{\hbar^2}{2mq_i^2} + \frac{m}{2}\dot{q}_i^2 + \frac{m\omega^2 q_i^2}{2}\right)N_i\right]$$
$$+4\nu\sqrt{N_1N_2}q_1q_2\frac{\left(q_1^2+q_2^2\right)\cos\left(\theta_{\text{tot}}+\theta_\nu\right) - \frac{m}{\hbar}\left(q_1^2q_2\dot{q}_2 + q_2^2q_1\dot{q}_1\right)\sin\left(\theta_{\text{tot}}+\theta_\nu\right)}{\left(q_1^2+q_2^2\right)^2 + \frac{m^2}{\hbar^2}\left(q_1^2q_2\dot{q}_2 + q_2^2q_1\dot{q}_1\right)^2}$$
$$+\frac{\gamma_1+\gamma_2}{4\pi}\left(\frac{N_1^2}{q_1^2}+\frac{N_2^2}{q_2^2}\right) + \frac{\gamma_1-\gamma_2}{2\pi}\frac{N_1N_2}{q_1^2+q_2^2}, \tag{4.7.1}$$

with $\theta_{\text{tot}} = \theta_1 + \theta_2$. To derive the equations of motion we use the projection method analogous to Subsection 4.6.2. We derive that the equations of motion are

$$\hbar\dot{N}_i = -\frac{2\alpha N_i}{1+\alpha^2}\frac{\partial\epsilon}{\partial N_i} + \frac{1}{1+\alpha^2}\frac{\partial\epsilon}{\partial\theta_i}, \tag{4.7.2a}$$
$$\hbar\dot{\theta}_i = \frac{1}{2}m\dot{q}_i^2 - \frac{1}{2}mq_i\ddot{q}_i - \frac{1}{1+\alpha^2}\frac{\partial\epsilon}{\partial N_i} - \frac{\alpha}{2N_i\left(1+\alpha^2\right)}\frac{\partial\epsilon}{\partial\theta_i}, \tag{4.7.2b}$$
$$mN_i\ddot{q}_i == -\frac{\partial\epsilon}{\partial q_i} + \frac{m}{2\hbar}\dot{q}_i\frac{\partial\epsilon}{\partial\theta_i} - 2\alpha\hbar N_i\frac{\dot{q}_i}{q_i^2}. \tag{4.7.2c}$$

Where we have used the same arguments for the EoM for q_i as we have used in Subsection 4.6.2 for the EoM for q to drop higher order time derivatives and to be able to interpret the damping term as a friction term. By making the EoM dimensionless we obtain

$$\dot{N}_i = -\frac{2\alpha N_i}{1+\alpha^2}\frac{\partial\epsilon}{\partial N_i} + \frac{1}{1+\alpha^2}\frac{\partial\epsilon}{\partial\theta_i}, \tag{4.7.3a}$$
$$\dot{\theta}_i = \frac{1}{2}\dot{q}_i^2 - \frac{1}{2}q_i\ddot{q}_i - \frac{1}{1+\alpha^2}\frac{\partial\epsilon}{\partial N_i} - \frac{\alpha}{2N_i\left(1+\alpha^2\right)}\frac{\partial\epsilon}{\partial\theta_i}, \tag{4.7.3b}$$
$$N_i\ddot{q}_i = -\frac{\partial\epsilon}{\partial q_i} + \frac{1}{2}\dot{q}_i\frac{\partial\epsilon}{\partial\theta_i} - 2\alpha N_i\frac{\dot{q}_i}{q_i^2}. \tag{4.7.3c}$$

4.7.1 Symmetric condensates

First consider the situation with the system symmetric, i.e. $q_1(0) = q_2(0)$, $N_1(0) = N_2(0)$ and without pumping. This system is identical with that considered in Subsection 4.6.4 if we would replace Γ_{in} by $\Gamma_{\text{in}} + \frac{1}{2}\Gamma_{\text{ex}}$, with $\Gamma_{\text{ex}} = \frac{m(\gamma_1-\gamma_2)}{\pi\hbar^2}$. When we add pumping to the system, we can still add up the interactions in the same way. In Fig. 4.8 the regions for values of the damping and the pumping where the systems are stable and where they are

unstable are depicted. In comparison with the regions in Fig. 4.7 we notice that for the diagrams labeled with (b), (c) and (e) the boundary line between the two regions no longer runs through the origin. From diagrams (b) and (c) we read off that the systems with small damping still remain stable for higher values of the pumping compared to the diagrams (b) and (c) in Fig. 4.7. The diagram labeled with (e) in Fig. 4.8 shows a small stable region for low damping, $\alpha < 0.1$ and low pumping but for a system with higher damping, around $\alpha = 0.1$, and equal pumping it would be unstable. This result is disputable, because one would expect that higher damping would cause the density of magnons to be lower, hence not shift a stable system to an unstable system. The boundary lines in diagrams (b), (c) and (d) are all monotonously increasing as where the lines in Fig. 4.8. Indicating that for higher damping the system becomes more stable, with an exception for diagram (e) for values of the damping, $\alpha < 0.1$.

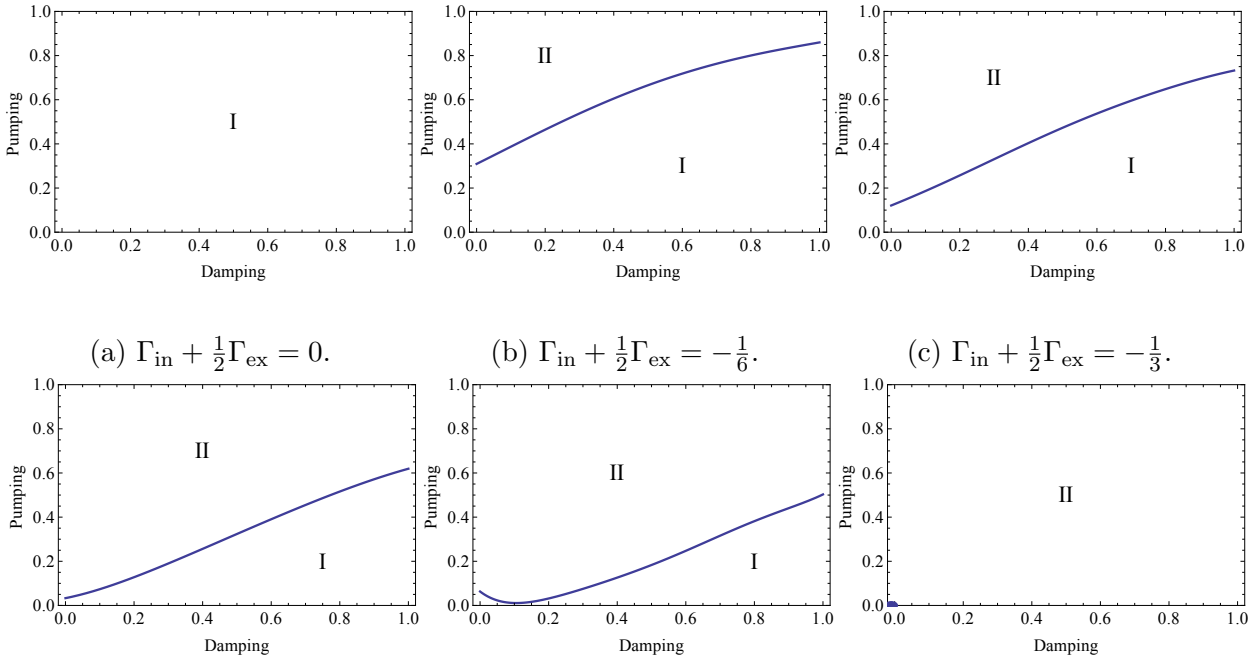

(a) $\Gamma_{\text{in}} + \frac{1}{2}\Gamma_{\text{ex}} = 0$. (b) $\Gamma_{\text{in}} + \frac{1}{2}\Gamma_{\text{ex}} = -\frac{1}{6}$. (c) $\Gamma_{\text{in}} + \frac{1}{2}\Gamma_{\text{ex}} = -\frac{1}{3}$.

(d) $\Gamma_{\text{in}} + \frac{1}{2}\Gamma_{\text{ex}} = -\frac{1}{2}$. (e) $\Gamma_{\text{in}} + \frac{1}{2}\Gamma_{\text{ex}} = -\frac{2}{3}$. (f) $\Gamma_{\text{in}} + \frac{1}{2}\Gamma_{\text{ex}} = -\frac{5}{6}$.

Figure 4.8: The regions of values for the damping and the pumping for which the system is stable, I, and for which the system is unstable, II.

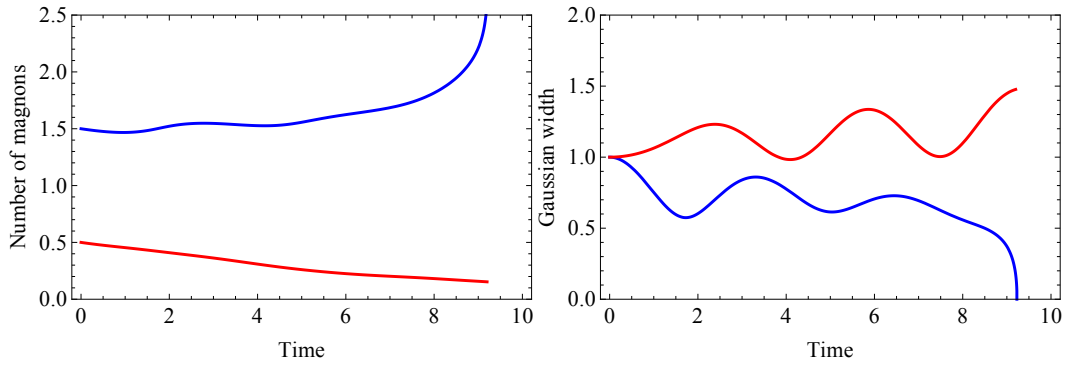

(a) (b)

Figure 4.9: In (a) and (b) are plotted the number of magnons and the Gaussian width, respectively, against the time, ωt, with $\Gamma_{\text{in}} = -\frac{1}{2}$, $\Gamma_{\text{ex}} = \frac{1}{2}$, $\alpha = 0.05$ and $\nu = 0.01$.

4.7.2 Asymmetric condensates

We consider a system which is not symmetric. In the situation where $\Gamma_{\text{ex}} = 0$ and $\nu = 0$ the system behaves like two independent condensates, which both behave as the BEC described in Subsection 4.6.4.

In general there is a multitude of parameters that influence the system, among which: Γ_{in}, Γ_{ex}, α, ν, $N_1(0)$, $N_2(0)$, $q_1(0)$ and $q_2(0)$. A full analyses of the system would be rather extensive due to the high number of parameters, hence we limit ourselves to considering a specific case which shows characteristics different from the systems we have considered in this thesis so far. In Fig. 4.9 the number of magnons and the Gaussian widths are depicted for a system with two asymmetric condensates. The system becomes unstable because the condensate with a relatively higher number of magnons at $t = 0$, indicated by the blue line, collapses. The condensate with a lower number of magnons at $t = 0$, indicated by the red line, does not seem to collapse. Unfortunately our model does not allow us to describe the behavior of the system after one of the two condensates has collapsed. That the number of magnons increases in the already more populated condensate and that the number of magnons decreases in the less populated condensate can be explained from the value of Γ_{ex}. In eqn. (4.7.1) we see that the term multiplying Γ_{ex} goes with $N_1 N_2$, which maximizes for $N_1 = N_2$ and minimizes if the magnons shift from the already less populated condensate to the more populated condensate.

Chapter 5

Conclusion

We have studied the stability of magnon BEC's in YIG at room temperature, which were realized in the experiment of Ref. [6]. First, in Chapter 2, we derived the magnon quantum many-body Hamiltonian up to fourth order in the magnon operators. We calculated that there are attractive interactions, hence deduced that it is possible for the condensate to be unstable. In Chapter 3 we made an estimate of the critical density by partially following a calculation as was done in [8]. In Chapter 4 we studied the effects of dynamics on the BEC by using a Gaussian ansatz. We specifically focused on the influence of the Gilbert damping and the parametric pumping and determined for several different cases if the condensate would be stable or not.

For studying the dynamics we derived equations of motion for the functions introduced by using the Gaussian ansatz. What the best method to obtain the equations of motion is, is not totally clear. The equation of motion for the Gaussian width was obtained partially based on physical intuition but a mathematically more rigorous method is desirable. The extension of the variational principle including the Rayleigh dissipation functional for the equations of motion for the wavefunctions, given in eqn. (4.5.5), to the Gaussian functions is failing, but why is not well understood. It is difficult to directly apply the theoretical model studied in this thesis to the experiments performed [6], because values for several parameters amongst which the interaction strengths and Gaussian widths are unknown.

It is interesting for future research to look for numerical solutions of the equations of motion for the wavefunctions describing the BEC's, instead of introducing a variational ansatz, deriving equations of motion for the variational parameters and look for numerical solutions of those as we have done. This approach would allow for comparison with experiment [6] more naturally than our approach does. It would also be interesting to study the

relaxation process by which pumped magnons relax into magnons forming the BEC. This would allow for a better understanding of the effect of the parametric pumping on the stability of the magnon BEC. Another possible focus for future research could be to obtain a better understanding of the methods used for the derivation of the equations of motion in the variational ansatz.

Bibliography

[1] S. N. Bose. Plancks gesetz und lichtquantenhypothese. *Z. Phys*, 26(178), 1924.

[2] A. Einstein. Quantentheorie des einatomigen idealen gases. *Sitzungsber. Kgl. Preuss. Akad. Wiss.*, 22(261), 1924.

[3] A. Einstein. Quantentheorie des einatomigen idealen gases, zweite abhandlung. *Sitzungsber. Kgl. Preuss. Akad. Wiss.*, 1(3), 1925.

[4] M.H. Anderson, J.R. Ensher, M.R. Matthews, C.E. Wieman, and E.A. Cornell. Observation of bose-einstein condensation in a dilute atomic vapor. *Science*, 269(5221), 1995.

[5] T. Holstein and H. Primakoff. Field dependence of the intrinsic domain magnetization of a ferromagnet. *Physical Review*, 58(1098), 1940.

[6] S.O. Demokritov, V.E. Demidov, O. Dzyapko, G.A. Melkov, A.A. Serga, B. Hillebrands, and A.N. Slavin. Bose-einstein condensation of quasi-equilibrium magnons at room temperature under pumping. *Nature*, 443(7110), 2006.

[7] V.V. Kruglyak, S.O. Demokritov, and D. Grundler. Magnonics. *Journal of Physics D: Applied Physics*, 43(264001), 2010.

[8] I.S. Tupistyn, P.C.E. Stamp, and A.L. Burin. Stability of bose-einstein condensates of hot magnons in yttrium iron garnet films. *Physical Review Letters*, 100(257202), 2008.

[9] R.A. Duine and H.T.C. Stoof. Explosion of a collapsing bose-einstein condensate. *Physical Review Letters*, 86(11), 2001.

[10] A. Kreisel, F. Sauli, L. Bartosch, and P. Kopietz. Microscopic spin-wave theory for yttrium iron garnet films. *European Physical Journal B*, 71(59), 2009.

[11] J. Hick, F. Sauli, A. Kreisel, and P. Kopietz. Bose-einstein condensation at finite momentum and magnon condensation in thin film ferromagnets. *European Physical Journal B*, 78:429–437, 2010.

[12] A.C. Swaving. *Spin transport and dynamics in antiferromagnetic metals and magnetic insulators*. PhD thesis, Utrecht University, 2012.

[13] R. M. White. *Quantum theory of magnetism*. third edition, 2007.

[14] B.A. Kalinikos and A.N. Slavin. Theory of dipole-exchange spin wave spectrum for ferromagnetic films with mixed exchange boundary conditions. *Journal of Physics C*, 19(7013), 1986.

[15] R.E Troncoso and Á.S. Núnez. Josephson effects in a bose-einstein condensate of magnons. *Annals of Physics*, 346, 2014.

[16] R.A. Duine. *Spintronics*. 2007.

[17] R.A. Duine and H.T.C. Stoof. Stochastic dynamics of a trapped bose-einstein condensate. *Physical Review A*, 65(13603), 2001.